LAWRENCE
LIVERMORE
NATIONAL
LABORATORY

LLNL-TR-829848

Development of Analytical Method for Measuring U and Pu Particles by Laser Ablation MC-ICP-MS for the NWAL

J. Wimpenny, P. Sotorrio, K. Samperton

December 8, 2021

Disclaimer

This work performed under the auspices of the U.S. Department of Energy by Lawrence Livermore National Laboratory under Contract DE-AC52-07NA27344.

Safeguards Technology Development Program
FY2021 Final Report
24 November 2021

WBS # – Project Title: 24.1.3.4 - Development of Analytical Method for Measuring U and Pu particles by Laser Ablation MC-ICP-MS for the NWAL

HQ Team Lead and PM: Arden Dougan & Ning Xu

Summary Statement of Work: This project will develop methodology to identify and analyze U and Pu containing particles using laser ablation MC-ICP-MS. The proposed work will involve: i) setup and optimization of the LA-MC-ICP-MS system, ii) testing and validation by analysis of QC standards, iii) designing analytical protocols for single particles, and iv) developing a data processing system. Ultimately, this project will output a detailed operating procedure documenting the experimental techniques and data processing routines required to perform particle identification and analysis by laser ablation MC-ICP-MS.

Report Title: Characterization of U isotope ratios by laser ablation MC-ICP-MS for IAEA Safeguards

Names of Authors and Affiliations: PI - Josh Wimpenny, Pedro Sotorrio, Kyle Samperton, Lawrence Livermore National Laboratory.

Major Highlights: 1) Setup and optimization of laser ablation MC-ICP-MS hardware complete at end of Q1. 2) Tests to assess the precision and accuracy of U isotopic analysis complete at end of Q2. 3) Method development to optimize the isotopic analysis of U-particles complete at end of Q4. 4) Development of user-friendly app to reduce laser ablation data from glass and particle materials complete at end of Q4.

Progress: See following report.

Table of Contents

Table of Figures

Table of Tables

1. Executive Summary

The FY21 project aim is to develop a capability to identify and analyze U containing particles using laser ablation MC-ICP-MS. In this report, we detail efforts to setup and optimize the laser ablation MC-ICP-MS hardware (Section 4), assess the accuracy and precision of the technique using in house U-glass standards (Section 5), develop methods to analyze micron-scale U particles (Section 6) and develop a data reduction package to reduce laser ablation data and assign appropriate uncertainties to final isotope ratios (Section 7). The instrument operating procedure and the accompanying data reduction package will be transferred to the IAEA.

2. Mission Relevance

STR 385: T.2.R6 - Develop and implement methods to detect signatures of nuclear activities in environmental samples
STR 393: SGAS-002 - Environmental Sample Analysis Techniques, "Implementation of the laser ablation-inductively coupled plasma mass spectrometry (LA-ICP-MS) technique to analyze Pu and mixed U/Pu particles in environmental samples"

3. Laser Ablation Mass Spectrometry

3.1. Introduction

Laser ablation systems are used as in-situ sample introduction systems for inductively coupled plasma mass spectrometers (ICP-MS). The basic principle is that a solid sample is placed in the laser sampling chamber, the laser energy is focused onto the sample surface and ablates the analyte, generating a fine aerosol that is carried to the ICP-MS plasma in a stream of carrier gas (usually helium). Analyte atoms in the sample aerosol are ionized in the plasma and the ions that are generated are transported through the mass spectrometer where the element of interest is selected based on the mass to charge ratio. Finally, the selected species is detected when it hits the detector array, usually comprised of ion counters and/or Faraday cups.

For high precision isotopic analysis by ICP-MS, the ideal method is to use an instrument with multiple detectors (multi-collector ICP-MS or MC-ICP-MS) to detect different isotopes of an element simultaneously. This overcomes the inherent instability of the plasma source while also negating problems associated with analyzing a transient laser ablation signal. The relative instability of the ablation signal means laser ablation MC-ICP-MS cannot produce isotope ratio data that is as precise as analysis made by traditional methods (i.e. sample in solution). Nevertheless, the ability to make relatively high precision isotope ratio measurements in-situ, with little or no sample preparation t means it could potentially be a powerful analytical technique for actinide isotope determination in nuclear safeguards.

This project addresses the mission needs listed in the IAEA *Development and Implementation Support Programme for Nuclear Verification 2020-2021* STR 393, SGAS-002 - Environmental Sample Analysis Techniques, "Implementation of the laser ablation-inductively coupled plasma mass spectrometry (LA-ICP-MS) technique to analyze Pu and mixed U/Pu particles in environmental samples".

In this report, we document the standing up of an MC-ICP-MS (Thermo Scientific Neptune-Plus) coupled with an excimer laser system (Photon Machines Analyte, 193nm) at Lawrence Livermore National Laboratory (LLNL) for in-situ actinide isotopic analysis, with a focus on uranium (Figure 1). We will document the initial setup of hardware and quality control testing of U isotope measurements in glass standards, before focusing on analytical methods to characterize the isotopic composition of U particles. In parallel with the analytical setup, we will also describe efforts to develop methods to export, reduce and finalize the isotopic data produced during laser ablation analysis.

Figure 1 – Neptune-Plus MC-ICP-MS (left) and Photon Machines 193nm excimer laser system (right) at LLNL.

3.2. Hardware Description

3.2.1. Mass Spectrometer: Thermo Scientific Neptune-Plus MC-ICP-MS

The Neptune-Plus MC-ICP-MS at LLNL is equipped with 10 Faraday detectors, 3 full-size secondary electron multipliers (SEMs) and 3 compact discrete dynode detectors (CDD's). This detector configuration is designed for isotopic analysis of uranium, enabling large ion beams of the major uranium isotope (^{238}U) to be measured on a Faraday detector and minor isotopes to be measured using ion counters (Figure 2). The ability to switch between an ion counter (IC2) and Faraday detector (L5) means that it is also straightforward to handle samples with variable ^{235}U enrichment levels. Energy filters (or RPQ's) on IC1 and IC3 help to reduce scattering of ions and peak tailing that might affect accurate analysis of ^{234}U and ^{236}U.

Table 1 – Detector configuration on the Neptune-Plus MC-ICP-MS for U isotope analysis

Detector

	L4	IC1B	L5/IC2	IC3	CDD5
Uranium isotopes	^{238}U	^{236}U	^{235}U	^{234}U	^{233}U
Amplifier Resistor	10^{11}	N/A	$10^{11}/10^{12}$	N/A	N/A
RPQ	N/A	Yes	No	Yes	No

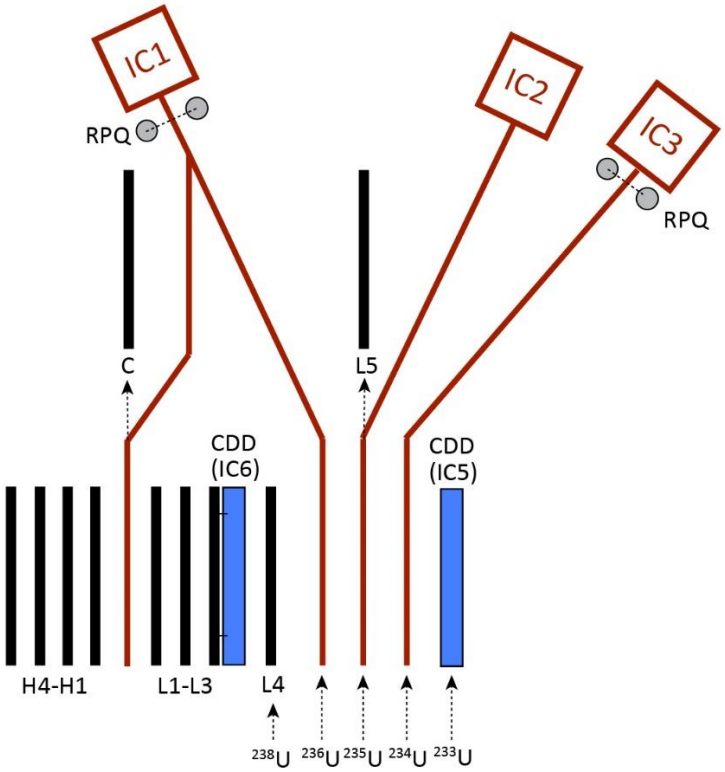

Figure 2 – The detector array on the Neptune-Plus MC-ICP-MS. Faraday detectors are in black, SEM's are in red, and CDD's are in blue. The IC1 and IC3 SEM's are fitted with energy filters (RPQ's). The U species and associated detectors are labeled.

3.2.2. Laser ablation system: Photon Machines Analyte 193nm excimer laser

The Photon Machines Analyte's 193nm excimer laser system has a 4ns pulse length. It has advantages over solid state laser systems with longer wavelengths such as the Nd:YAG 213nm or 266nm systems because the 193nm laser energy couples better with IR transparent materials. Its relatively short pulse length reduces thermal effects of laser interaction with the sample surface (e.g., isotopic fractionation associated with kinetic processes), although not to the extent of newer, femtosecond laser systems. The system at LLNL is equipped with a two-volume laser cell, also termed the 'Helex' cell (Figure 3). The sample cell is a chamber in which the sample is housed and in which the ablation is performed. The cell is filled with helium carrier gas and ablated aerosol is transported out of the cell to the plasma-source on the ICP-MS. The dual volume cell has significant advantages over the older single volume model as its design eliminates the occurrence of spatial fractionation effects within the chamber and enhances response rate and washout time (i.e., the time between stopping ablation and the signal dropping to background values).

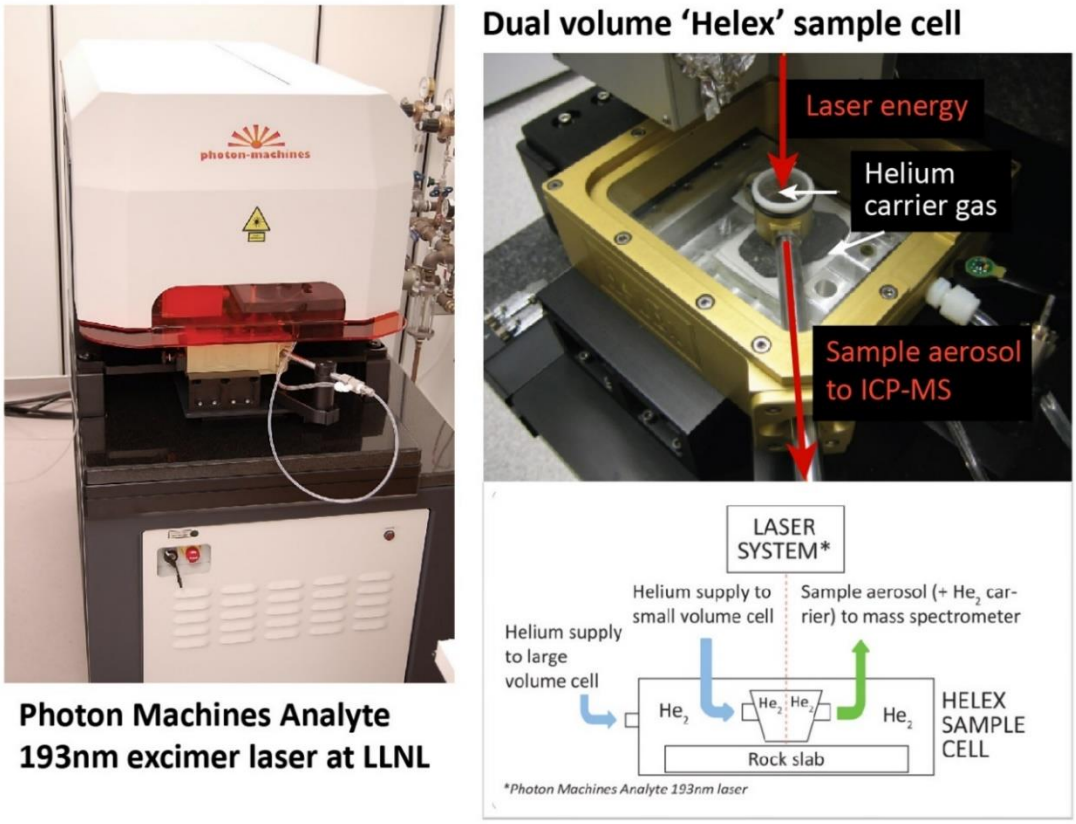

Figure 3 – The dual volume 'Helex' sample cell on the laser ablation system. Helium is supplied to both the main cell and inner cup as a carrier gas for the ablated sample aerosol, which is transported out of the cell to the ICP-MS.

4. Setup and Optimization of Laser Ablation MC-ICP-MS at LLNL

4.1. Basic Hardware Configuration

Testing of the hardware configuration aimed to ascertain the setup that produced the highest precision isotope ratio data. Higher sensitivities, lower oxide production and more stable ion beams typically produce higher quality data and thus were selected for during testing. The instrument and laser parameters used during testing are summarized in Table 2. To test signal stability and sensitivity several glass standards were ablated over the course of this work. The NIST glass standards 610 and 612 have U concentrations of ~460 and 37 ppm respectively, with highly depleted $^{235}U/^{238}U$ ratios of 0.00238 (Duffin et al., 2015). The USGS glass standard GSD-1G has a U concentration of ~40 ppm and a depleted $^{235}U/^{238}U$ ratio of 0.00369 (Jochum et al., 2011). Because these samples contain depleted uranium, most of the analyses were performed with ^{235}U on IC2, although some limited testing was also performed with ^{235}U on L5. We anticipate that switching between IC2 and L5 will be important in future studies where samples with variable ^{235}U enrichment levels are analyzed.

The laser system is supplied with helium carrier gas to the Helex cell. Flow rates of 0.6 l/min to the main cell and 0.5 l/min to the smaller sample cup were found to give relatively rapid response time from the start of ablation to the detection of ions on the mass spectrometer. The sample aerosol is carried in high purity helium to the mass spectrometer, where it is mixed with a flow of argon (termed the 'sample gas' flow) before hitting the plasma source (Figure 4). The sample gas flow rate was tuned for maximum sensitivity at between 0.9-1.05 l/min. Higher sample gas flow rate often increased the sensitivity but also generated higher percentages (from 3-20%) of U-oxide. Changes in the oxide abundance did not change the measured $^{235}U/^{238}U$ ratio, but further testing will be required to ascertain whether higher oxide generation (and potentially other polyatomic species) could affect the measurement of minor U isotopes.

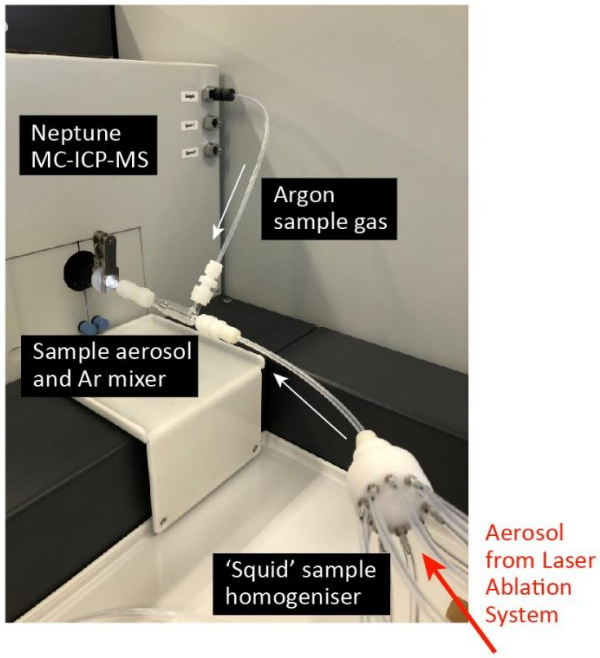

Figure 4 – The sample introduction setup. Aerosol is transported from the laser system through a sample smoothing device ('squid') before mixing with Ar 'sample gas' before the aerosol hits the plasma.

The Neptune hardware required minimal testing; the torch and injector types and auxiliary argon gas flows are typically constant and do not affect the instrument response. Uranium isotope analyses have been performed on a regular basis in solution mode using the Neptune at LLNL, so the cup configuration and instrument tune parameters were already optimized. We also have a long-term record of the instrumental mass bias factor and ion counter-Faraday gain factors for isotopic analysis of uranium reference standards in solution. The applicability of these factors to the accurate isotopic analysis of uranium by laser ablation is described further in Section 5. The most important hardware changes are the sample and skimmer cones used on the Neptune's front end. The Neptune can be fitted with high sensitivity cones ('Jet' sampler and 'X' skimmer) which increase sensitivity over the standard ('H') cones, the downside being that they can also increase oxide production and degrade the low-resolution peak shape. However, in testing the ablation of NIST 610 we were able to obtain an increase in sensitivity by a factor of ~10 using the high sensitivity setup, while keeping oxide levels below <5% and a flat-topped U-peak. Thus, all tests in this report were performed using the high-sensitivity cones. Ultimate sensitivity depends on a

combination of ICP-MS and laser parameters. Using a 50 µm spot size, frequency of 7Hz and fluence of 2.1 J/cm^2 we typically obtain a signal of 0.6-0.7 V ^{238}U from NIST 610.

Table 2 – Basic instrumental parameters used during the hardware setup.

Neptune MC-ICP-MS			*Photon Machines Analyte*
Sample cone	H/Jet	Helium 1 (main cell)	0.6 l/min
Skimmer cone	H/X	Helium 2 (inner cup)	0.5 l/min
Sample gas (Ar)	0.9-1.05 l/min	Spot size (microns)	40-85
Aux gas	0.8 l/min	Ablation Frequency	5-7 Hz
Cool gas	16 l/min	Fluence (J/cm^2)	2.1-3.8
Center mass	254.15		
Integration time	0.13-0.26s		
No. of integrations	200-400		
Resolution (m/Δm)	Low (400)		

4.2. Laser Ablation Analytical Protocol

Laser ablation analysis can be performed on a range of sample matrices (e.g. glass, particle) and range of ablation configurations (e.g. line, raster, spot). The laser energy and optics are co-focused, so focusing the optics on the sample surface also focuses the laser energy. During a spot analysis the laser drills down through the sample, and in doing so the amount of ablated material that reaches the plasma decreases with time. This is because the laser becomes progressively out of focus as the pit is excavated, and the ablated material is more difficult to mobilize out of the excavated laser pit. A characteristic decaying profile is produced during spot analysis, as illustrated in Figure 5a. Ablating lines and performing rastering scans avoid these problems and can, in theory, produce a stable ablation signal that mirrors the signal generated by aspirating a solution. However, these types of scans require a sample that has a large and compositionally homogenous area to produce meaningful data, which is not common in most natural samples. Because the ablation of micron scale particles will produce a short-lived transient signal it is most appropriate to test the laser ablation hardware by performing spot analysis.

A plot from a typical analysis of NIST 610 is shown in Figure 5. The method acquires data for ^{233}U, ^{234}U, ^{235}U, ^{236}U and ^{238}U but only data for ^{235}U and ^{238}U is presented here. A total of 200×0.26s integrations are made during each sample analysis, equating to a sampling time of ~50s. The first 20s of that data collection period is left with the laser off in order to characterize the instrumental background, which is subtracted from the final ablation signal. After 20s the laser fires, which is marked by a rapid increase in signal and followed by a steadily decaying signal for all isotopes. The isotope ratio measurements are taken from the most stable part of the curve, typically 2-5s after the start of ablation. To assess the various hardware options used here we have focused on the uncertainties associated with the measured ^{235}U/^{238}U ratio, although other isotope ratios were also calculated (see Appendix A and B for representative isotopic data for all three standards). All uncertainties are presented as 2× the standard error of the mean. For consistency, the average isotopic compositions for all samples were calculated using the final 100

measurements of each analysis (Figure 5b). Depending on the analytical parameters, the uncertainties generated for the $^{235}U/^{238}U$ ratio of NIST 610 ranged from 0.2-1.5% (2σ). For reference, internal uncertainties for $^{235}U/^{238}U$ ratios in reference standards measured in solution by the Neptune-Plus MC-ICP-MS at LLNL are <0.05%.

The IAEA recommended International Target Values (ITVs) for relative uncertainties associated with traditional solution MC-ICP-MS methods but have not recommended separate values for isotopic analysis by laser ablation (Zhao et al., 2010). The ITV for a ^{235}U abundance measurement by solution MC-ICP-MS is 0.7% for depleted uranium and 0.07% for HEU. Our testing indicates that raw $^{235}U/^{238}U$ ratios can be constrained to within 0.2% in a glass CRM by laser ablation MC-ICP-MS. However, this relative uncertainty does not incorporate corrections for mass bias and ion counter gains and is likely to be much larger for ablation of micron-sized particles. Recently reported relative uncertainties (1σ) for $^{235}U/^{238}U$ ratios in U particles measured by laser ablation MC-ICP-MS are between 1 and 4% (Donard et al., 2017; Ronzini et al., 2019; Craig et al., 2020), which may be a more realistic range to target during future development work.

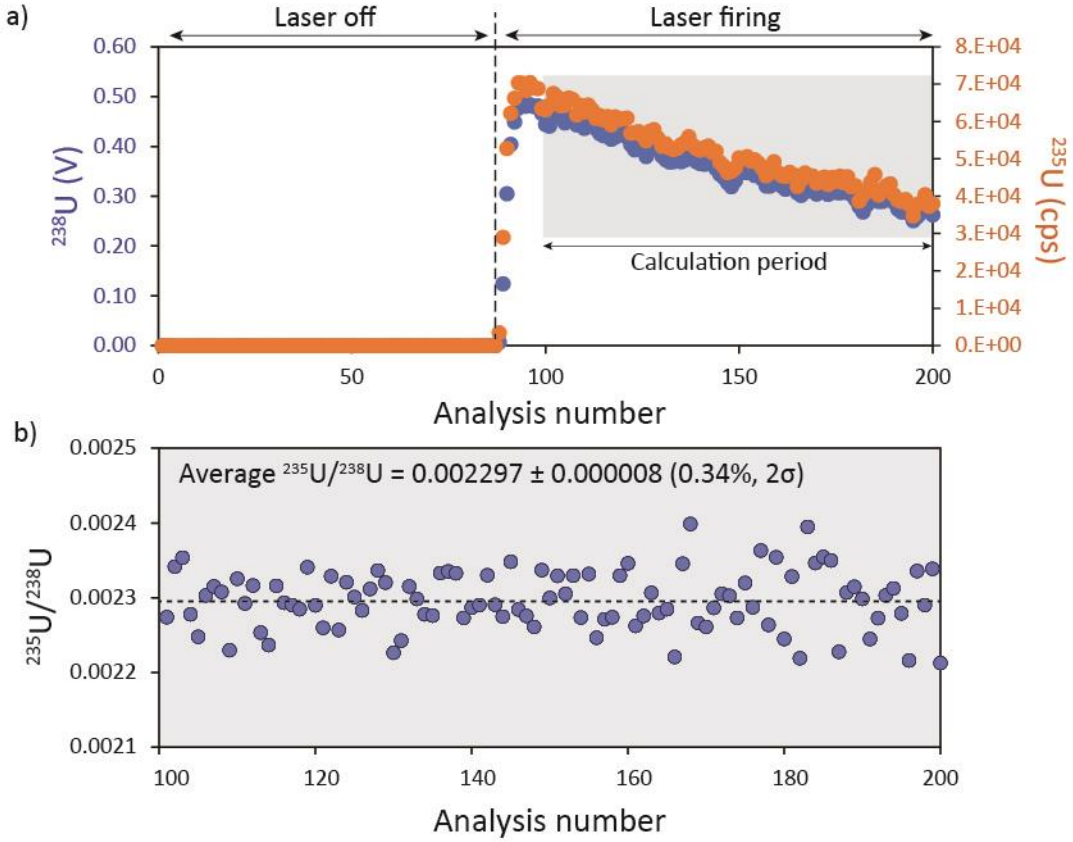

Figure 5 – A plot from an isotopic analysis of NIST 610 glass. The top plot (a) shows the intensities of ^{238}U (blue) and ^{235}U (orange) before and during ablation of the sample. Data was also collected for ^{233}U, ^{234}U and ^{236}U but is too low to show here. The shaded region in (a) shows the data used to calculate the $^{235}U/^{238}U$ isotope ratio shown in (b).

The precision of an isotope ratio measurement will decrease with signal intensity; thus, although analyses of NIST612 and GSD-1G were performed during testing the ~10× lower U concentration

in these materials doubled the uncertainties (Figure 6). This also means that changes in laser parameters that act to ablate more sample material (i.e., spot size, frequency, laser fluence) also increase the signal intensities and decrease uncertainties. These are less relevant when considering the ablation of micron scale particles, which are likely to be ablated by a single shot.

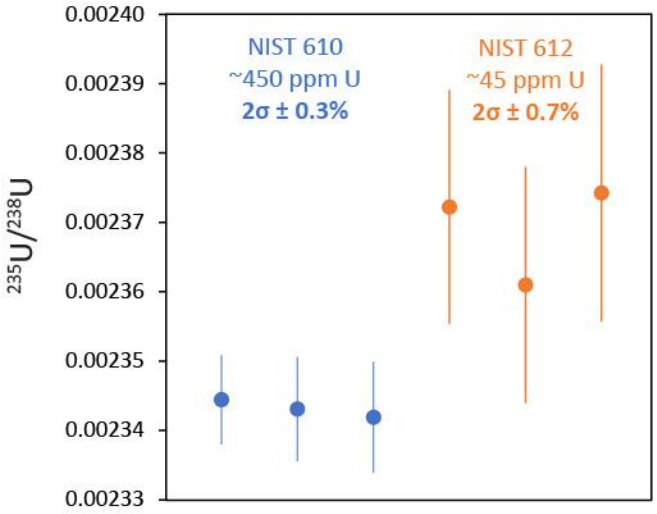

Figure 6 – A plot showing the difference in precision when analyzing the $^{235}U/^{238}U$ isotope ratio in NIST 610 and NIST 612, which have different U concentrations.

4.3. Optimizing the Laser Ablation Technique

4.3.1. Sample introduction from laser to ICP-MS

Because the sample aerosol is generated by discrete laser pulses the signal that reaches the plasma can exhibit instability that reflects the laser frequency (Figure 7). In addition to potentially affecting the precision of the isotopic analysis, studies have shown that at lower frequencies (<3-5Hz) this pulsing can produce a spectral skew affect (Muller et al., 2009) that can produce offsets in trace element data produced by laser ablation depth profiling. Thus, attempts have been made to smooth out the signal generated by laser ablation analysis to avoid this type of analytical artifact and produce a higher precision dataset. To this end, we tested the use of a signal smoothing device called a 'squid', as illustrated in Figure 7. The squid splits the sample aerosol into ten separate lines of varying lengths that then recombine prior to mixing with the Ar sample gas (Figure 4), producing a much smoother signal. However, although the laser plot was less noisy using this smoothing device, the isotope ratio measurements were, on average, not significantly improved over a standard inlet tube. This probably reflects the fact that multi-collection tends to overcome instabilities in signal generated by the plasma or the laser pulsing.

Ultimately, although any increase in precision appears to be tenuous, there is no reason not to use the squid in further testing; it clearly reduces noise generated by the laser pulsing and there is no reduction in signal intensity from ablation. We saw no change in background levels over the course of the analytical sequences, indicating that neither the squid nor the standard inlet tube imparts measurable memory effects. One question mark will be whether the squid remains beneficial during particle analysis. As individual particles may be ablated by a single laser pulse the associated signal will be extremely short lived. We predict that the squid will produce a slightly

longer, but lower intensity signal than the standard inlet tube. Testing performed in Section 6 aimed to assess any impact of the inlet tube configuration on precision.

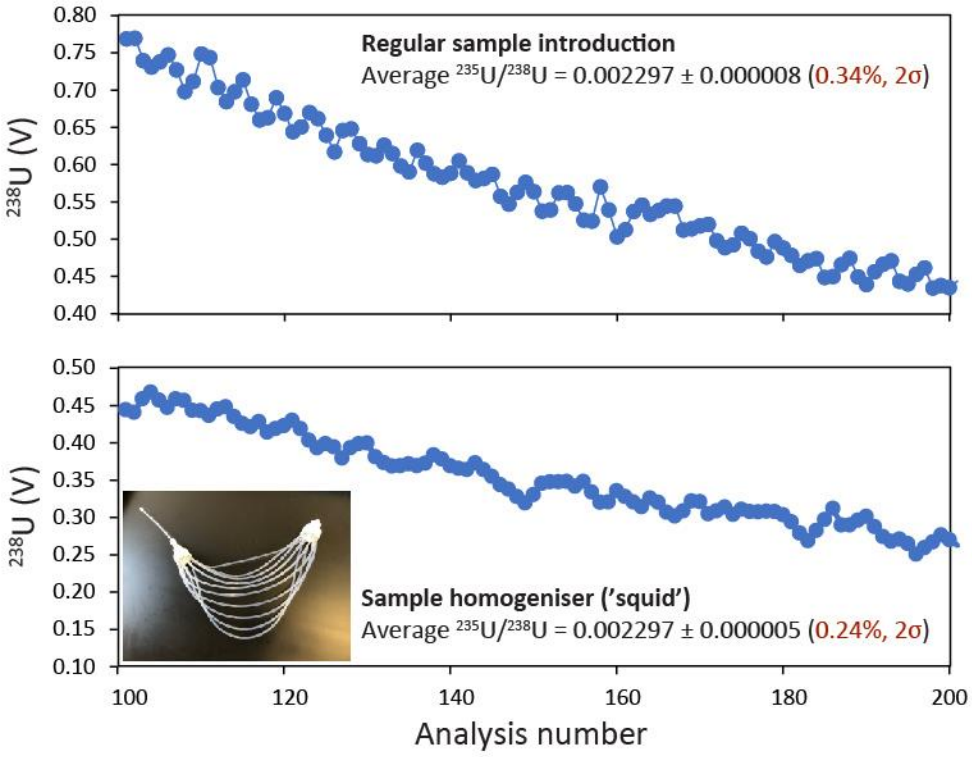

Figure 7 – Plot showing the effect of using a sample smoothing device ('squid') to eradicate instability from laser pulsing. In general, there was not a significant improvement in the precision of the $^{235}U/^{238}U$ ratio when using the squid.

4.3.2. Detecting ^{235}U using a Faraday (L5) or Ion Counter (IC2)

In samples with varying $^{235}U/^{238}U$ ratios it will be important to be able to switch between Faraday detector and ion counter. In general, a 1 mV signal on a Faraday cup is equivalent to 62415 cps on an ion counter, and signals of 10 mV or greater are more precisely measured by a Faraday detector. To test this, NIST 610 was analyzed with ^{235}U on the L5 Faraday and IC2 SEM (Figure 8). Spot sizes of 50 and 85µm were tested to generate ^{235}U signals of ~1 mV and 4 mV on L5. As shown in Figure 8a, signals of ~1 mV on L5 generate $^{235}U/^{238}U$ ratios with uncertainties of 1.1-1.5%, far less precise than comparable signals on IC2. Increasing the ^{235}U signal to 4 mV on L5 also increased the precision of the $^{235}U/^{238}U$ ratios to ~0.4%, approaching the measurement uncertainty using IC2 (Figure 8b). Based on these data, any ^{235}U signal of >5 mV should be placed on the L5 Faraday. The advantage of the Faraday detector is that the final $^{235}U/^{238}U$ ratio need only be corrected for mass bias effects whereas the $^{235}U/^{238}U$ ratio generated with ^{235}U on IC2 must also be corrected for the IC-Faraday gain, which imparts additional uncertainty. Furthermore, in unknown samples it may not be feasible to measure ^{235}U on an ion counter and risk saturating the detector. The downside is that the precision of isotopic analysis will suffer in samples with highly depleted ^{235}U contents.

The ion beam detected by the Faraday's produces a current that is converted into a voltage using high resistivity amplifiers. The Neptune has a virtual amplifier configuration in which there is the option of assigning a 10^{10}, 10^{11} or 10^{12} Ω resistor to any Faraday cup. As standard, the Faraday detectors are assigned with 10^{11} Ω resistors, but in theory the use of 10^{12} Ω resistors should be beneficial for the measurement of mV-level signals. However, as shown in Figure 8 the data obtained when assigning a 10^{12} Ω resistor to L5 (orange) does not produce higher precision data. Because the 10^{11} Ω resistor can be used at higher intensities, and potentially for samples with a wider range of ^{235}U enrichment levels, this type of resistor has been used throughout the development of the laser ablation capability (see Sections 5 and 6).

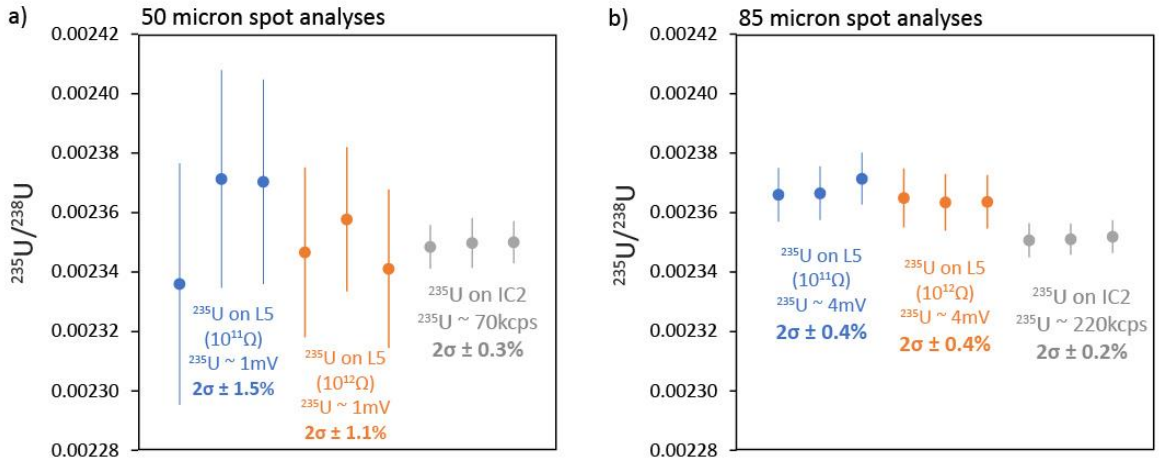

Figure 8 – Plot showing a comparison between measuring the ^{235}U signal on a Faraday detector (L5) and SEM (IC2). With a 1 mV signal the difference in precision between IC and Faraday was a factor of 4-5 (a). With a larger ^{235}U signal of ~4 mV the difference in precision decreased to a factor of ~2 (b). A correction factor of 1.019 for the IC2-Faraday gain was applied to the IC data.

4.3.3. Laser fluence

The laser fluence is a measurement of the energy delivered per unit area (in J/cm^2). At higher fluence more energy will be delivered to the sample surface and more material is ablated per pulse, resulting in higher signals delivered to the mass spectrometer. However, the laser will also drill down through the sample faster, resulting in a less stable signal with a steeper decay profile. To test whether changes in fluence inherently change the uncertainty associated with an isotopic analysis we performed a limited test on NIST 610 using fluences of 2.1 and 3.85 J/cm^2. These were combined with spot sizes of 50 µm and 40 µm respectively, to ensure that the intensities generated by the ablation matched. Using these ablation parameters, the uncertainties on the ^{235}U/^{238}U ratio were identical at ~0.24% (2σ), indicating that small differences in fluence do not change the uncertainty of the isotope ratio measurement. This is unlikely to change during ablation of micron-scale particles, where the sample is destroyed by a handful of laser pulses and any interaction between the laser energy and sample substrate is less important.

4.3.4. Guard Electrode

The platinum guard electrode (GE) sits between the quartz torch and load coil on the ICP-MS. Its purpose is to narrow the ion energy spread and produce higher ion transmission efficiencies (e.g. Xu et al., 2014) and thus it is typically turned on during ICP-MS analysis. However, it also increases the production of polyatomic species, meaning it can be problematic for some laser ablation studies. To test the importance of the GE a simple test was performed with the guard electrode turned on and off while all other laser ablation parameters were kept constant (50 µm spot, 7 Hz, 2.1 J/cm^2). When the GE was turned off the Ar sample gas flow had to be reduced from ~1.035 l/min to a new optimal level of 0.89 l/min. Oxide levels decreased with the GE off from 3-5% to negligible levels. Signal intensities also decreased by ~50% from previous levels (i.e. ~0.7V ^{238}U in NIST 610 to ~0.3V ^{238}U).

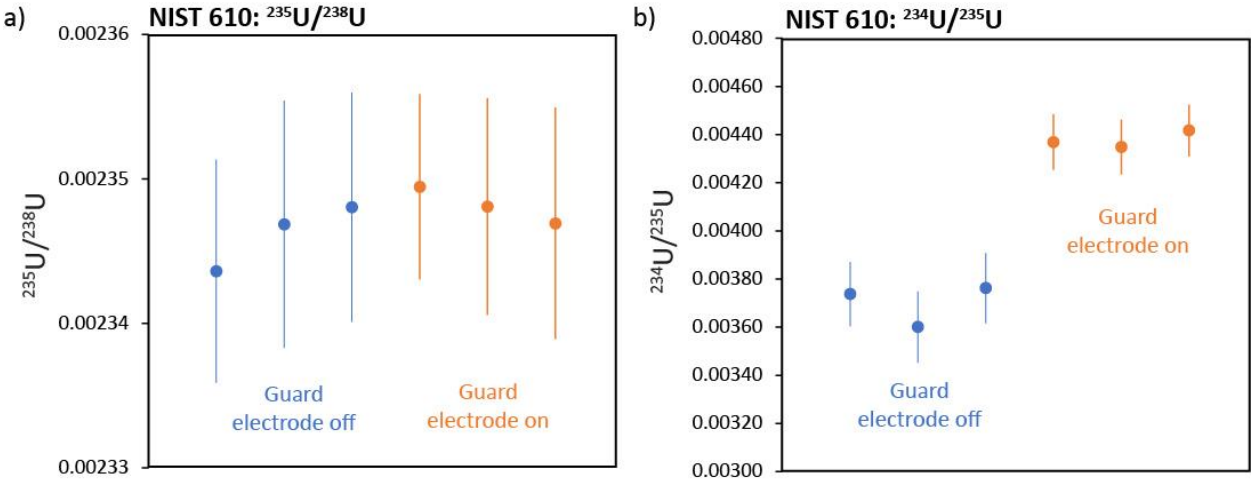

Figure 9 – Plot showing the comparison between performing analysis with the guard electrode on (orange) and off (blue). Although this makes no difference to the ^{235}U/^{238}U ratio (a) there is a significant shift in the ^{234}U/^{235}U ratio (b).

Isotopic analysis produced identical ^{235}U/^{238}U data with the GE on or off, and the isotope ratio data had similar precision (Figure 9a). However, for the ^{234}U/^{235}U ratio there were significant differences between data generated with the GE on or off (Figure 9b). Analysis performed with the GE off had lower ^{234}U/^{235}U ratios outside of analytical precision. Similar effects were also observed for NIST 612 and GSD-1G (see Appendix B). More testing would be needed to fully understand the cause of this shift. It is likely that polyatomic species such as ^{194}Pt^{40}Ar are less readily formed with the GE off, and these have a disproportionate effect on the minor isotopes of U such as ^{234}U. However, during testing in Section 5, we found that the raw ^{234}U/^{238}U and ^{236}U/^{238}U ratios were systematically closer to reference values with the GE on. Higher signal intensities also give better raw measurement uncertainties. For this reason, we defaulted to having the GE on during continued isotopic analysis in Sections 5 and 6.

5. Testing the accuracy and precision of U isotopic analysis by laser ablation MC-ICP-MS

5.1. Reference Materials

To test the accuracy of U isotopic analysis by laser ablation requires access to solid-form standard reference materials with known isotopic compositions. Glass standards are ideal for this purpose as they couple well with the laser energy and have a high degree of isotopic homogeneity. Most widely available reference materials, such as NIST and USGS glasses, have natural or depleted $^{235}U/^{238}U$ ratios and low abundances of minor U isotopes, which means they are inappropriate for testing the ability to measure samples with enriched isotopic compositions. For this reason, the testing performed here utilized a series of U-doped glasses that were prepared in house at LLNL from calcium-aluminum silicate base glasses (Knight et al., 2018). These have a variance in ^{235}U content from ~0.725% (natural uranium), ~50%, and ~93%, across three U concentrations from ~5, ~50, and ~500 ppm. The isotopic compositions of these glasses were previously characterized by dissolving small fragments (~10 mg) and analyzing in solution-mode by MC-ICP-MS at LLNL (Eppich et al., 2016, Knight et al., 2018) (Table 3). The wide range of isotopic compositions of these materials enables robust evaluation of our ability to characterize samples with variable ^{235}U enrichment factors.

Table 3 – Isotopic compositions of the 6 reference glasses analyzed in this study. Isotopic compositions taken from in house analysis by solution MC-ICP-MS unless otherwise stated (Eppich et al., 2016; Knight et al., 2018).

	$^{234}U/^{238}U$	Std Uncert (2σ)	$^{235}U/^{238}U$	Std Uncert (2σ)	$^{236}U/^{238}U$	Std Uncert (2σ)
CAS3-53-500	0.007995	0.000035	1.1240	0.0029	0.005639	0.000024
CAS3-94-500	0.1682	0.0018	15.91	0.16	0.05031	0.00054
CAS3-NAT-500	0.0000580	0.0000021	0.007936	0.000031	0.0000015	0.0000015
SAC-53-50	0.007806	0.000020	1.0985	0.0022	0.005498	0.000013
SAC-53-500	0.008017	0.000013	1.1283	0.0013	0.0056467	0.0000082
GSD-1G[a]	0.00001798	0.00000003	0.0036846	0.0000018	N/A	N/A
NIST 610[b]	0.00000945	0.00000005	0.00239555	0.00000047	0.00004314	0.00000004

[a]Jochum et al., (2011); [b]Zimmer et al., (2014)

5.2. Correcting for instrumental mass bias

There is an inherent bias present in the raw isotope ratios measured by mass spectrometers. In ICP-MS instruments, this is typically associated with the transfer of ions through the ion optics region of the mass spectrometer. Here, the lighter isotopes are preferentially deflected, leaving a population that is relatively enriched in heavy isotopes. This artifact, known as a mass bias effect, must be corrected to obtain accurate isotope ratio data. For isotope systems where internal normalization is not appropriate, this correction is usually performed by analyzing the isotopic composition of a standard reference material with known isotopic composition and using the difference between measured and true isotope ratios to calculate a mass bias correction factor that is applied to the unknowns. Because the extent of mass bias is not constant and will change between and within analytical sequences the mass bias correction factor must be calculated regularly within an analytical sequence. To obtain accurate U isotope ratio data by laser ablation

MC-ICP-MS requires the selection of an appropriate reference standard that contains sufficient U and high enough ^{235}U enrichment for both ^{235}U and ^{238}U to be measured on Faraday detectors. This prevents the additional uncertainty arising from cross calibration of ion counters. Furthermore, the reference material must be isotopically homogenous at the level of analytical precision (i.e. <0.2-0.4%). The in-house U glass standards have enriched ^{235}U compositions and high enough U concentrations (50-500 ppm) to be used as mass bias correction standards. However, their spatial heterogeneity could not be assessed by solution MC-ICP-MS. Instead, the U-glasses were analyzed using Secondary Ion Mass Spectrometry (NanoSIMS) at LLNL, and SIMS-Single-Stage Accelerator Mass Spectrometry (SIMS-SSAMS) at the U.S. Naval Research Laboratory (Knight et al., 2018). The average composition of multiple in-situ analyses are presented in Table 4 and the degree of isotopic heterogeneity is represented by the reproducibility of the analyses (in %).

Table 4 – Isotopic composition of 5 reference glasses measured in situ by NanoSIMS and SIM-SAMS. Here, the RSDs are used as a first order indictor of the isotopic heterogeneity within in each glass.

Sample	Technique	$^{234}U/^{238}U$	2σ	RSD	$^{235}U/^{238}U$	2σ	RSD	$^{236}U/^{238}U$	2σ	RSD
CAS-94-500	NanoSIMS	0.166603	0.022711	13.6%	16.19534	1.676335	10.4%	0.049957	0.005356	10.7%
	SIM-SAMS	0.1686	0.006083	3.6%	16.06051	0.268602	1.7%	0.050714	0.002338	4.6%
CAS-53-500	NanoSIMS	0.008026	0.000504	6.3%	1.139124	0.025083	2.2%	0.005541	0.000655	11.8%
	SIM-SAMS	0.007974	0.000123	1.5%	1.120241	0.004958	0.4%	0.005677	6.37E-05	1.1%
CAS-Nat-500	NanoSIMS	8.7E-05	5.7E-05	65.5%	0.008279	0.001014	12.2%	not measured		
	SIM-SAMS	5.95E-05	1.79E-05	30.1%	0.007915	0.000304	3.8%	3.47E-06	2.68E-06	77.3%
SAC-53-50	NanoSIMS	0.007734	0.002855	36.9%	1.078263	0.076112	7.1%	0.005974	0.002397	40.1%
	SIM-SAMS	0.007894	0.001556	19.7%	1.089784	0.03103	2.8%	0.005504	0.000748	13.6%
SAC-53-500	NanoSIMS	not measured								
	SIM-SAMS	0.00792	0.000257	3.2%	1.122397	0.021632	1.9%	0.005616	0.000419	7.5%

Based on these data, the U-glasses CAS-53-500 and SAC-53-500 are the most suitable materials to use as mass bias correction standards, with relative uncertainties associated with duplicate $^{235}U/^{238}U$ ratios ranging from 0.4-2.2%. To further assess the suitability of these reference glasses as mass bias standards, we made 20 isotopic analysis of U in CAS-53-500 and SAC-53-500 by laser ablation MC-ICP-MS. The analyses were performed systematically in a grid across ~2mm chips of each standard, with ^{238}U and ^{235}U intensities of >100mV. The raw $^{235}U/^{238}U$ ratios are plotted in Figure 10. Systematic drift in the $^{235}U/^{238}U$ ratio of CAS-53-500 is likely caused by drift in the instrumental mass bias rather than sample heterogeneity. Regardless, this simple test indicates that both standards have spatially homogeneous U isotope ratios with relative uncertainties on the $^{235}U/^{238}U$ ratio of <0.1%. Because CAS-53-500 has been more thoroughly characterized by solution MC-ICP-MS this was ultimately chosen as the best standard to use for mass bias corrections during glass analysis (Section 5) and development of particle characterization methods (Section 6).

During each analytical sequence, the CAS-53-500 glass was analyzed multiple times as a verification standard. Each sequence was set up with the same structure, in which 6 ‘unknowns’ were bracketed by CAS-53-500 and mass bias factors were calculated for the unknowns from the measured $^{235}U/^{238}U$ ratio of the standards. The uncertainty associated with the $^{235}U/^{238}U$ ratios of

the bracketing standards were propagated into the final isotopic compositions of the unknowns. The significance of this uncertainty is dependent from how well each isotope ratio can be measured. This is discussed further in Section 5.5.

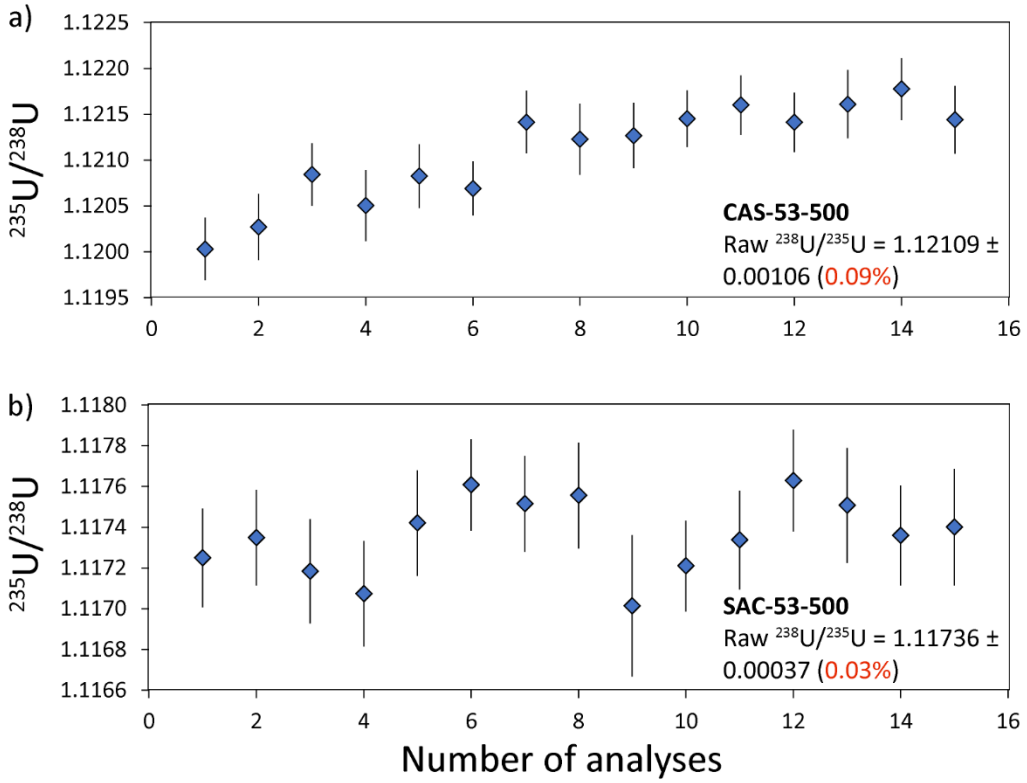

Figure 10 – The raw $^{235}U/^{238}U$ ratios of replicate analyses of CAS-53-500 (a) and SAC-53-500 (b) by laser ablation MC-ICP-MS. The 2σ relative uncertainty associated with these analyses is <0.1%, indicating isotopic homogeneity at the spatial scale of these analyses.

5.3. Ion Counter Gain Corrections

The minor isotopes of U (^{233}U, ^{234}U and ^{236}U) are present at relatively low abundances in most samples, meaning they must be detected using ion counters. Because the response of ion counters to an ion beam varies and is not necessarily equivalent to the signal produced on a Faraday detector, the ion counters must be calibrated to obtain accurate isotope ratio data. The offset between the response of the ion counter and the signal generated on a Faraday detector (assuming 1mV = 62415 cps) is called the ion counter gain. We tested two methods to calculate the ion counter gain factors during this study. The first used ion counter gain factors calculated during solution MC-ICP-MS analysis over the past 3 months. These are termed the 'assumed' gain factors. Whereas the instrumental mass bias must be calibrated daily and is highly sensitive to changes in the running parameters (e.g. sample gas flow), the ion counter gains are generally more stable within and between analytical sequence. The advantage of calculating the gain factors by solution MC-ICP-MS is that the measurement is more stable and relative uncertainties are smaller. Also, we can apply half-mass baseline correction to account for peak tailing of major isotopes onto ion counters,

which cannot be performed by laser ablation. The disadvantage is that although the gain factors are relatively stable over the long term, in-run drift does still occur, as do small variations in gain factor between each analytical sequence. The alternative method is to perform the gain correction online, i.e. using laser ablation analysis of CAS-53-500 to calculate ion counter gain factors during sample-standard bracketing. These are termed 'interpolated' gain factors. This overcomes any drift in gain factors within and between runs, but the half mass baseline measurements that are used to correct for tailing effects cannot be performed. In addition, because ^{235}U is measured by Faraday collector this method cannot be used to calculate the ion counter gain factor for ^{235}U on IC2.

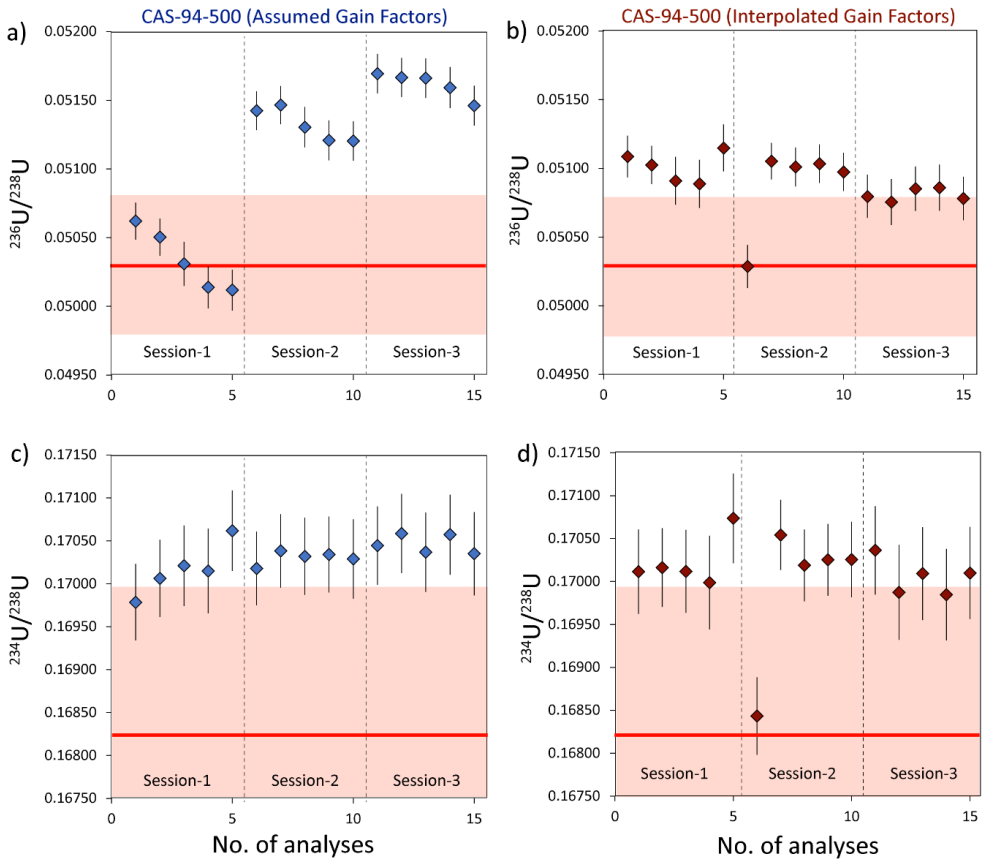

Figure 11 – The $^{236}U/^{238}U$ (a, b) and $^{236}U/^{238}U$ (c,d) ratios of the reference glass CAS-94-500. The ratios in a) and c) were calculated using assumed gain factors. The ratios in b) and d) were calculated using interpolated gain factors.

To establish the optimal method of gain factor correction we directly compared data calculated by both techniques for CAS-94-500 (Figure 11). As shown, when calculating the $^{236}U/^{238}U$ ratio using an assumed gain factor there is significant drift in the isotope ratio between analytical sequence outside of the 1σ analytical precision (Figure 11a). In contrast, using the interpolated gain factor results in more reproducible $^{236}U/^{238}U$ ratios within and between analytical sequence (Figure 11b). This indicates that the gain factor on IC1 is not stable at the degree of precision of our isotopic analysis. Interestingly, the $^{234}U/^{238}U$ ratio is far less sensitive to whether assumed or interpolated gains are used during the data reduction process (Figure 11c, d). This likely indicates a discrepancy

in performance between IC3 and IC1 over the long term. Ultimately, because interpolated gain factors gave a significant improvement in the $^{236}U/^{238}U$ data we used this correction method for all ^{236}U and ^{234}U data. Because CAS-53-500 has subequal ^{235}U and ^{238}U levels we could not use it to calculate an interpolated IC gain factor for measurement of ^{235}U on IC2. For samples with low-levels of ^{235}U (i.e. samples with natural or depleted $^{235}U/^{238}U$ ratios) the ^{235}U gain correction was calculated from an assumed value measured by solution MC-ICP-MS.

5.4. Isotopic Analysis of U in Reference Glasses

Six of the seven U reference glasses (excluding CAS-53-500) were each analyzed 15 times by laser ablation MC-ICP-MS over 3 analytical sequence. In each case, the mass bias and gain factors for IC1, IC3 and IC5 were calculated using the measured composition of CAS-53-500. The experimental setup used the basic parameters presented in Table 2 and described in Section 4 (i.e. 50µm spot size, 7Hz repetition rate, fluence ~2 mJ/cm^2). The instrument was tuned so that the ablation of NIST-610 produced a ^{238}U signal of 0.5-0.7V. The average results of these analyses and the % difference between our measured values and reference values are presented in Figure 12-14 and Tables 5 and 6. In the following, we summarize the most important observations from these isotopic analyses.

5.4.1. Glass standards with natural or depleted ^{235}U contents

Three of the reference glasses have natural or depleted ^{235}U contents: NIST 610, GSD-1G and CAS-Nat-500. The $^{235}U/^{238}U$ ratios were reproducible between and within analytical sequences with RSDs <0.5% for all samples. However, the $^{235}U/^{238}U$ ratios were all systematically lower than the reference values by between 0.4 and 1.7% (Figure 12, 13a, Table 5).

Table 5 – Average U isotope ratios measured in the three reference glasses with natural or depleted ^{235}U contents.

	$^{234}U/^{238}U$	2σ	RSD (%)	Offset (%)	$^{235}U/^{238}U$	2σ	RSD (%)	Offset (%)	$^{236}U/^{238}U$	2σ	RSD (%)	Offset (%)
CAS3-NAT-500	0.0000631	0.0000025	3.88	8.9	0.007882	0.000021	0.27	-0.7	0.0000051	0.0000020	39.6	231.7
GSD	0.0000447	0.0000088	19.68	148.7	0.003670	0.000017	0.45	-0.4	0.0000496	0.0000075	15.2	N/A
NIST 610	0.0000107	0.0000004	3.51	13.4	0.0023544	0.0000032	0.14	-1.7	0.0000445	0.0000005	1.20	3.3

Because ^{235}U was measured using an ion counter (IC2) we hypothesize that the relatively low $^{235}U/^{238}U$ values reflect a small discrepancy between the assumed and true gain factors. A relatively small shift in this gain factor by ~1% would shift the $^{235}U/^{238}U$ of these glasses to within uncertainty of their reference values. This highlights the drawback in using an assumed gain factor for calculating isotope ratios, particularly when the offset between assumed and true factors is greater than precision of the isotopic analysis. Robust characterization of the ion-counter gain factor, for example by using a secondary standard with ^{235}U measured on IC2, would be required to correct for small offsets in the $^{235}U/^{238}U$ ratio. Of course, the ultimate goal of this project is to characterize the isotopic composition of U in micron scale particles; if their $^{235}U/^{238}U$ ratios can only be constrained to 5-10% (e.g. Pointurier et al., 2011; Craig et al., 2020) then such small offsets in the ion counter gain factor become largely irrelevant.

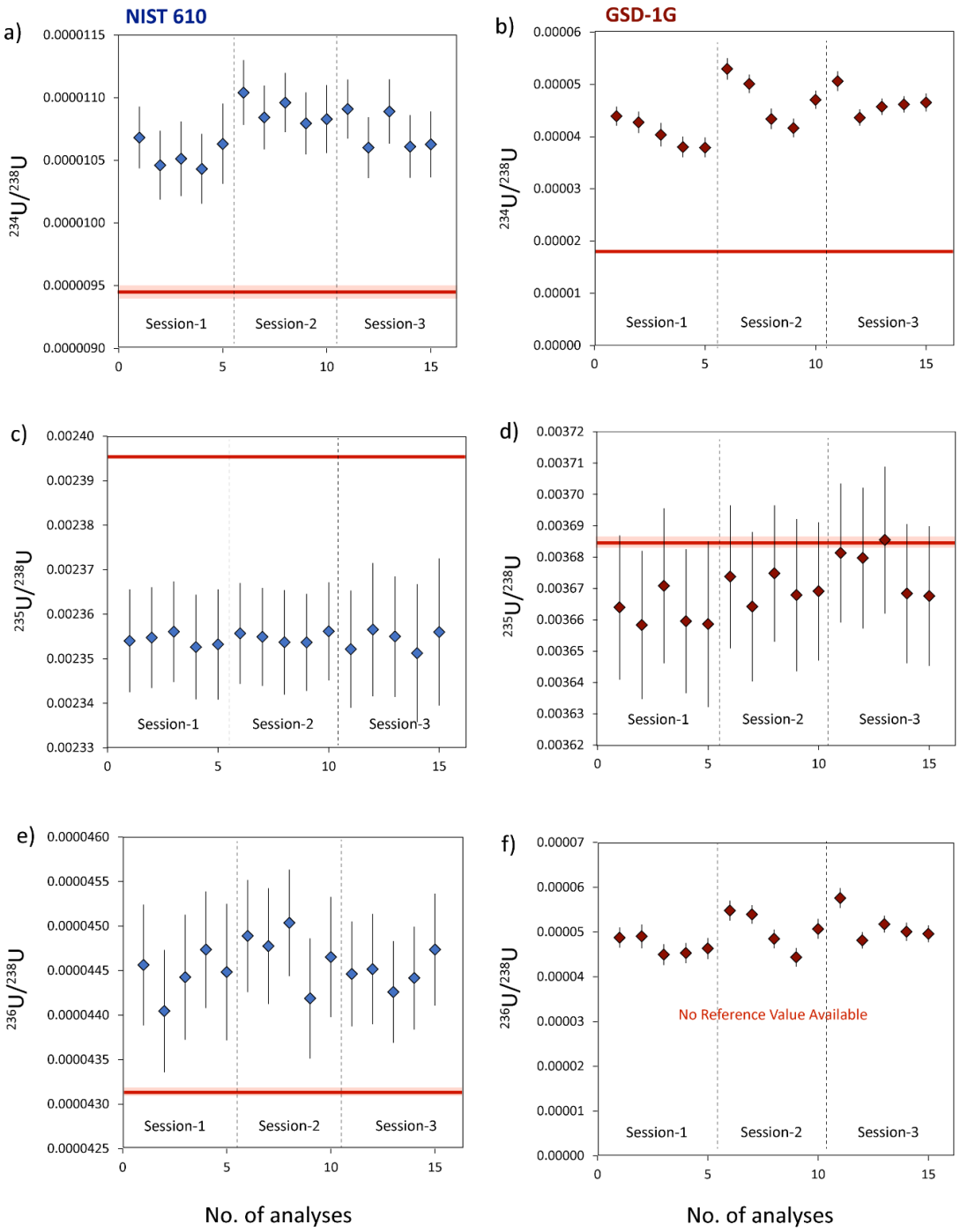

Figure 12 – Uranium isotope systematics in NIST 610 and GSD-1G. Reference values and 2σ uncertainties are shown in red. Error bars on individual data points are 2σ and incorporate mass bias, ion counter gain and measurement uncertainties.

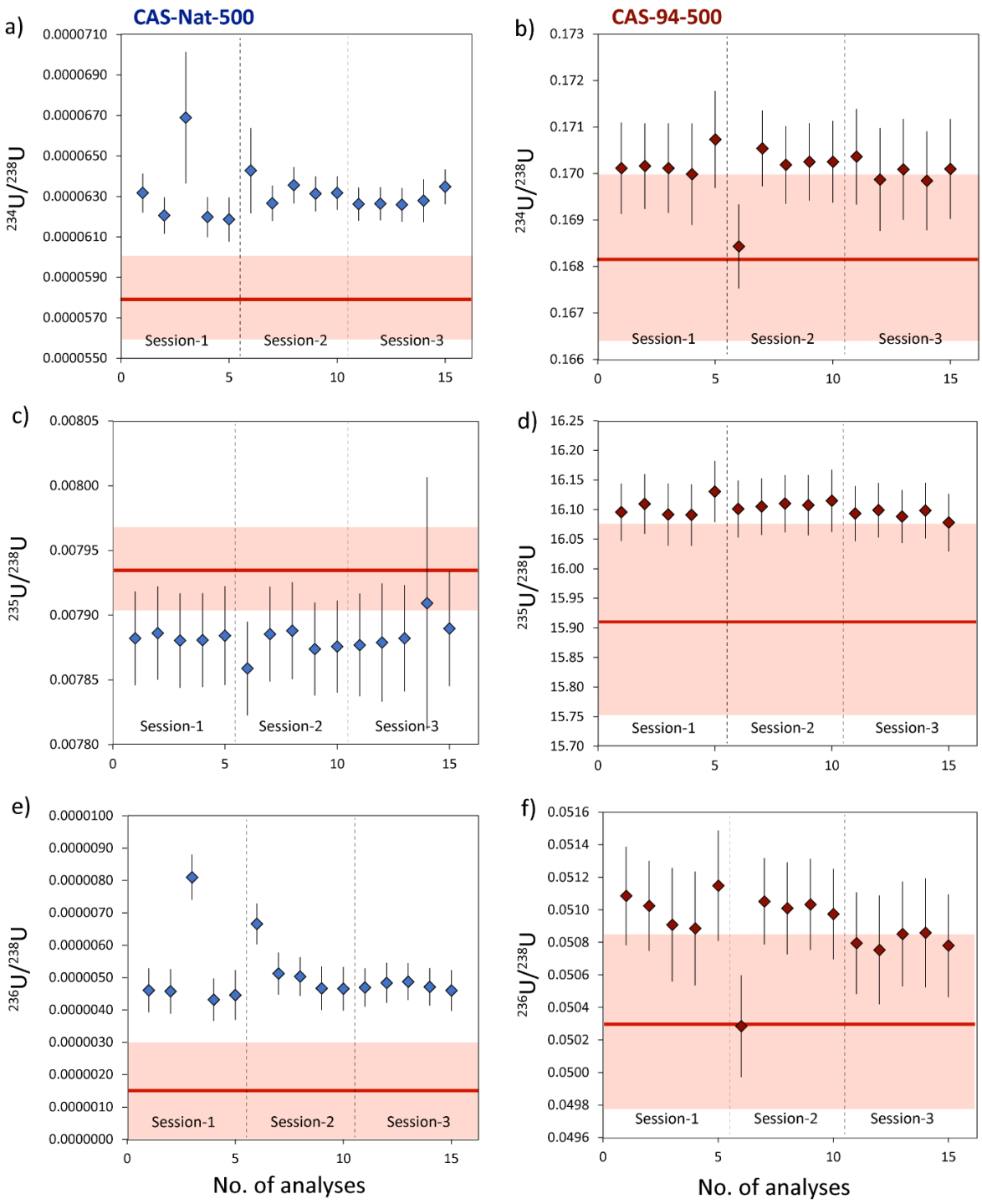

Figure 13 – Uranium isotope systematics in CAS-Nat-500 and CAS-94-500. Reference values and 2σ uncertainties are shown in red. Error bars on individual data points are 2σ and incorporate mass bias, ion counter gain and measurement uncertainties.

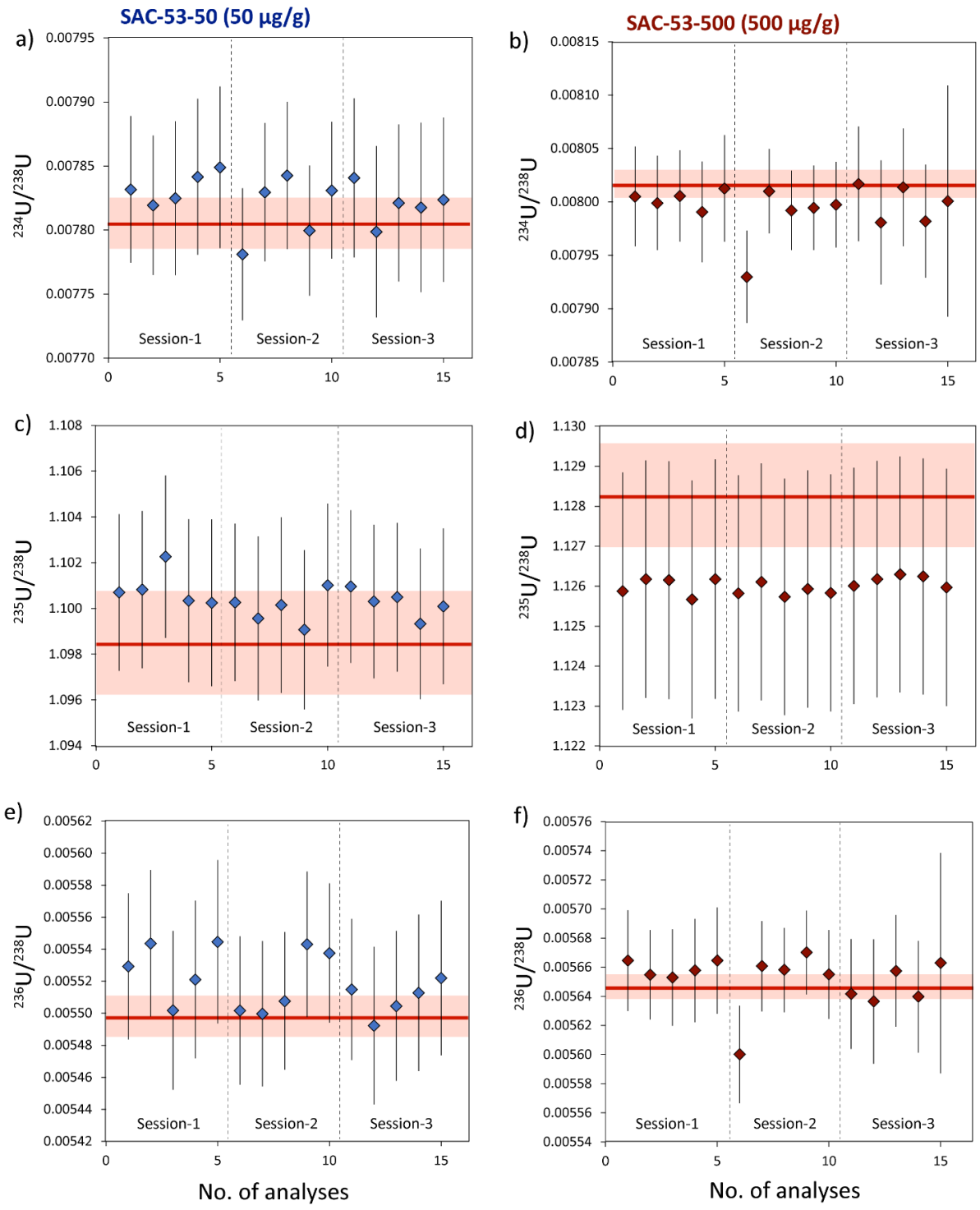

Figure 14 – Uranium isotope systematics in CAS-53-50 and CAS-53-500. Reference values and 2σ uncertainties are shown in red. Error bars on individual data points are 2σ and incorporate mass bias, ion counter gain and measurement uncertainties.

The $^{234}U/^{238}U$ and $^{236}U/^{238}U$ ratios were less reproducible than the $^{235}U/^{238}U$ ratio within and between analytical sequence, with RSDs between 1.2 and 39.6%. This relative instability is due to

the fact that ^{234}U and ^{236}U are present at ~2 orders of magnitude lower than ^{235}U. The relatively low abundances of ^{234}U and ^{236}U also means that their isotope ratios are highly sensitive to the presence of polyatomic interferences and/or peak tailing effects from the major isotope (^{238}U) into ^{236}U. This can explain why the $^{234}U/^{238}U$ and $^{236}U/^{238}U$ ratios are systematically elevated above reference values (Table 5). NIST 610 is a synthetic glass with >50 trace elements doped into the matrix at ~450ppm. The USGS glass standard GSD-1G is similarly doped with trace elements to ~50ppm but has a basaltic matrix to more closely mimic natural rock samples (Jochum et al., 2011). The trace element composition of CAS-Nat-500 has not been characterized but it was synthesized from a calcium-silicate precursor under conditions that could have introduced trace element contaminants. For all three glasses, elements such as lead and platinum in the matrix can form polyatomic interferences in the MC-ICP-MS that directly interfere at the uranium masses. For example, NIST-610 is well known to have an elevated platinum content due to its preparation in a platinum-rhodium lined furnace (Duffin et al., 2013) and the polyatomic species $^{194}Pt^{40}Ar^{+}$ and $^{196}Pt^{40}Ar^{+}$ are potential interferences on ^{234}U and ^{236}U respectively. Our results illustrate the challenge with obtaining highly accurate and precise ^{234}U and ^{236}U data by in situ techniques in samples with variable trace element impurities and depleted ^{235}U contents. However, this may not be significant for safeguards samples as such concentration of platinum in NIST 610 is unlikely to be present in U particles on swipes.

5.4.2. U-glass standards with enriched ^{235}U contents

The three U-glasses CAS-94-500, SAC-53-50 and SAC-53-500 have elevated $^{235}U/^{238}U$ ratios, with higher ^{235}U contents corresponding to higher abundances of ^{234}U and ^{236}U (See Table 6 for compositions). The higher count rates generated during ablation improves the counting statistics and renders polyatomic interferences less important, meaning we obtain more accurate and precise U isotope ratios.

Table 6 – Average U isotope ratios measured in three reference glasses with enriched ^{235}U contents.

	$^{234}U/^{238}U$	2σ	RSD (%)	Offset (%)	$^{235}U/^{238}U$	2σ	RSD (%)	Offset (%)	$^{236}U/^{238}U$	2σ	RSD (%)	Offset (%)
CAS3-94-500	0.1701	0.0010	0.60	1.1	16.101	0.025	0.16	1.2	0.05090	0.00041	0.81	1.2
SAC-53-50	0.007823	0.000037	0.48	0.2	1.1004	0.0015	0.14	0.2	0.005518	0.000035	0.64	0.4
SAC-53-500	0.007995	0.000042	0.53	-0.3	1.12601	0.00039	0.03	-0.2	0.005652	0.000034	0.61	0.1

As presented in Table 6, the isotope ratios generated by laser ablation match the reference values to within ~1%, and RSDs of the 15 replicate analyses are typically better than 1%. The highest precision and most accurate data were produced from the SAC-53-50 and -500 glasses, which generated data that matched the reference values to within 0.5%. There was no clear difference in data quality between the 50 ppm and 500 ppm glass. The glass with the highest ^{235}U enrichment, CAS-94-500, yielded U isotope ratios that are systematically ~1.2% higher than the reference values. We hypothesize that this offset reflects variable contamination of the CAS-94-500 sample aliquots during the chemical purification procedure prior to solution mode analysis. Even a small amount of natural U or LEU would have had a significant effect on the composition of such an

isotopically enriched sample. This is illustrated in Figure 15 where the $^{235}U/^{238}U$ values are plotted vs $^{234}U/^{238}U$ for both laser ablation and solution data. The isotopic data from solution analysis form a well constrained mixing line between a highly ^{235}U enriched endmember and low ^{235}U enriched contaminant, with the laser ablation data lying in a cluster at the highly enriched end. This illustrates one of the major benefits of U isotopic analysis by laser ablation; there is no addition of U blank that could alter the final U isotope ratio.

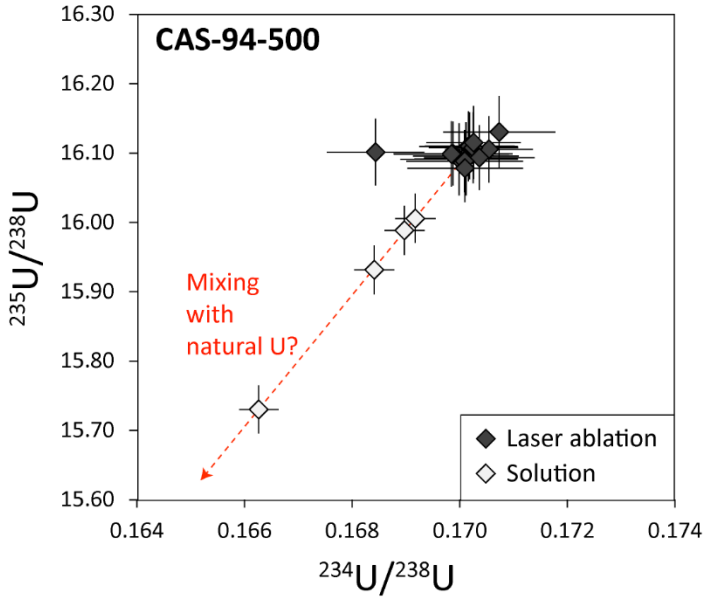

Figure 15 – The U isotope systematics in samples of CAS-94-500 measured by solution and laser ablation MC-ICP-MS. A clear mixing line extends from the laser ablation measurements to the solution analysis, indicating a mixing between HEU and less enriched contaminant. Uncertainties are 2σ.

Ultimately, the data described in Section 5.4. show that we have successfully setup a laser ablation MC-ICP-MS system that can obtain accurate and precise U isotope data in glass substrates for a wide range of U isotope ratios. The $^{235}U/^{238}U$ ratio is relatively easy to measure, even in samples with depleted ^{235}U contents and relative uncertainties equating to 0.1-0.5% are achievable. Presumably, the ablation of micron-scale particles will generate relatively low count rates, together with a highly transient signal, which may be detrimental to the data quality and uncertainties associated with final isotope ratios. However, the relatively robust $^{235}U/^{238}U$ data obtained here indicate that we should also expect to obtain accurate $^{235}U/^{238}U$ ratios from U-particles, albeit with much lower precision. As one would expect, the measurement of minor U isotopes (^{234}U and ^{236}U) by laser ablation is challenging, even in U-rich glasses. Testing described in Section 6 will enable us to assess whether it is also possible to obtain robust isotopic data for the minor U isotopes from micron scale U-particles.

5.5. Isotope ratio uncertainties

The final uncertainties associated with the isotopic data are a product of several factors: the measurement itself, the reproducibility of the mass bias and ion-counter gain standard and how precisely the reference value of that standard is known. This last factor is a critical component of the final combined standard uncertainty (CSU); it constrains the lowest possible uncertainty that can be achieved in the theoretical scenario where no uncertainty is associated with the sample analysis and correcting standards.

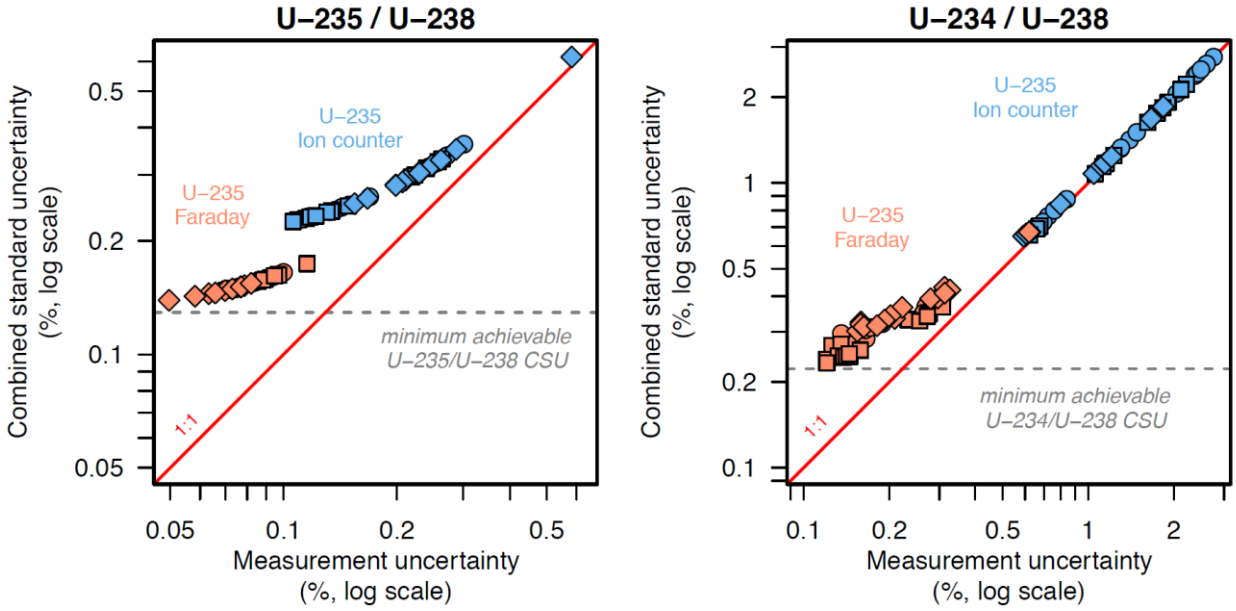

Figure 16 – Relationship between the measurement uncertainty and final combined standard uncertainty. The minimum achievable CSU is based on the uncertainty of the reference standard. Data points in blue represent those where ^{235}U was measured by ion-counter.

In Figure 16 we show the relationship between the measurement uncertainty and final CSU for $^{235}U/^{238}U$ and $^{234}U/^{235}U$ analyses of the reference glasses. The 1:1 line represents the case where the final CSU is equal to the measurement uncertainty, i.e. any uncertainties associated with the normalizing standard are negligible. The data in red were collected with ^{235}U on a Faraday detector (enriched ^{235}U) and the data in blue were collected with ^{235}U on an ion counter (depleted ^{235}U). The data in red tend towards the theoretical lowest possible CSU. In other words, the final uncertainties are largely controlled by the uncertainty on the mass bias/gain factor standard rather than the measurement uncertainty. This indicates that when ^{235}U could be analyzed on a Faraday collector our analyses are close to optimal; changes in data collection or experimental parameters would not greatly improve the final precision of these analyses. Better constraints over the isotopic composition of U in CAS-53-500 would be required to improve these data. The data in blue are closer to the 1:1 line, indicating that the measurement uncertainty is dominant, probably due to low count rates in glass samples with depleted U isotopic compositions. Irrespective of the isotopic composition, we expect the particle analysis to generate even lower count rates meaning the quality of the isotopic data will almost certainly be constrained by the particle measurement itself. It follows that factors controlling the data quality of the reference glasses, such as the mass bias and

ion counter gain factors, will be a negligible source of uncertainty during the isotopic analysis of U particles.

6. Developing techniques to analyze micron-scale U-particles by laser ablation MC-ICP-MS

6.1. Introduction to particle analysis

Solid samples such as glasses are a best-case scenario when performing isotopic analysis by laser ablation. The medium is relatively homogenous and glass thicknesses far exceed the depth at which the laser will excavate during a single spot analysis. This means the resulting signal is long-lived and relatively consistent, producing isotopic data that can be reduced easily and has relatively high precision (< 0.5% RSD). In contrast, the analysis of particles by laser ablation is challenging for several reasons. First, the optics provided on most laser ablation systems are optimized for spot sizes of 20-100µm, which makes identifying micron or sub-micron scale objects difficult (Figure 17). Second, due to the small size of the particles the signal resulting from ablation may also be too small to resolve either by Faraday detector or ion counter. Moreover, any signal produced will be short lived and highly unstable compared to ablation of a glass, making resulting data relatively imprecise. The challenge here is to test the effectiveness of the 193nm excimer laser system in ablating micron scale U-particles and assess the precision and accuracy of the resulting data using reference materials.

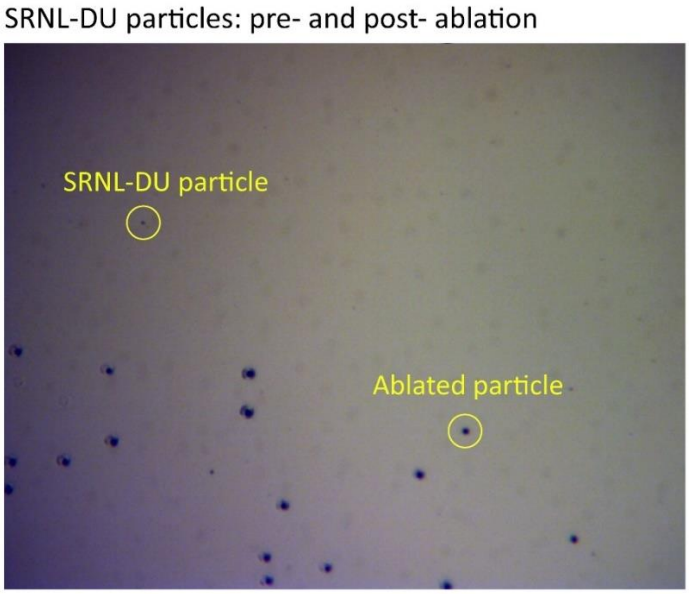

Figure 17 – Image of SRNL-DU particles pre- and post-ablation. For reference, the DU-particles are approximately 1 micron in diameter.

6.2. Reference materials

To test the ability of the laser ablation MC-ICP-MS setup at LLNL to make U-isotopic analysis of particles required material with a known isotopic composition to test on. To this end we used two different standard materials; an in-house dispersion of NIST SRM U200 and depleted uranium particles that were provided to us by Savannah River National Laboratory (SRNL). We used U200 for initial method development and benchmarked the method with the SRNL-DU sample. . The isotope ratios of the reference materials are provided below in Table 7. Note, that the minor isotope abundances of the SRNL-DU were not previously constrained and we were provided with a nominal ^{235}U content of <0.2%.

Table 7 – U isotope ratios in the U200 reference standard previously characterized by solution MC-ICP-MS (Richter et al., 2003) and the depleted uranium sample from SRNL that was characterized using SIMS (Scott et al., 2021)

Standard ID	**$^{235}U/^{238}U$**	**2σ**	**$^{234}U/^{238}U$**	**2σ**	**$^{236}U/^{238}U$**	**2σ**
U200	0.25119	0.00025	0.0015661	0.0000021	0.0026549	0.0000019
SRNL-DU	0.00173	0.00010	0.0000068	0.0000035	0.0000807	0.0000086

6.3. Experimental setup

The setup of the laser ablation system and mass spectrometer were identical to the setup for glass analysis (see Section 4). Initial testing found no significant difference between using the ‘squid’ signal smoothing device or a regular inlet tube between the laser ablation system and the mass spectrometer. Ablation parameters such as the laser frequency, fluence and integration time were also varied during testing but produced no systematic differences in data quality. The relative insensitivity of particle data to changes in laser parameters likely stems from the limited ablation period and the fact that the signal produced is highly unstable, irrespective of the parameters controlling the ablation process.

The structure of the analytical sequence for particle analysis was also configured similarly to the glass standards in Section 5, with unknowns bracketed by reference standards for calculation of mass bias and ion counter gain factors. Although the use of a particle reference standard would ensure similar ablation characteristics between standard and sample, we opted to use the glass standard CAS-53-500 for mass bias corrections instead. This is for several reasons; i) the lack of suitable particle reference materials outside of the test samples studied here, ii) the fact that CAS-53-500 is already well characterized by solution and laser ablation techniques, iii) we assume that the precision of U isotope data obtained for U-particles will be relatively low (1-5%) meaning the use of a matrix matched mass bias standard may not greatly improve the final data quality. Although CAS-53-500 was used here, any well characterized reference glass could serve as a suitable correction standard for safeguards purposes.

In initial testing, individual particles of U200 were identified prior to starting each sequence and data for each particle was collected in its own file, which was then reduced separately. This technique was time consuming and, because the laser ablation optics were not designed to resolve micron scale objects, sometimes lead to misidentification of U-particles. An alternative method to identify and ablate U-particles is by rastering the laser over a set area and collecting the data in a single data file. In this way data for multiple U-particles can be collected rapidly with little or no time required to identify the location of samples. We anticipate that the rastering method will be the most useful for future applications by the IAEA. However, both methods were developed during testing, and both methods are compatible with being reduced by the LARA package (Section 7). Data presented here for U200 (and later on for SRNL-DU) will be from a combination of individual particles analyses and rastering experiments, as the data quality produced is equivalent.

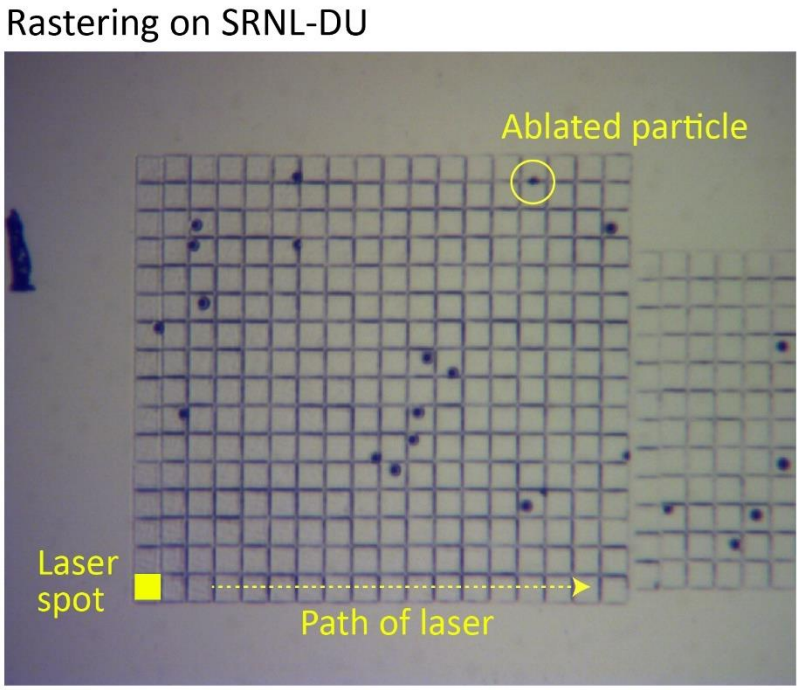

Figure 18 – Image showing the SRNL-DU silicon planchet after rastering the laser over a 0.5mm x 0.5mm square. Each spot had a dose of 3 laser pulses. Ablated particles are clearly visible after rastering is complete.

The U200 reference material is a powder and the in-house preparation of the U200 laser sample involved dispersing an aliquot of the powder by pipetting a slurried solution in ethanol onto a silicon planchet. Characterizing the size of the particles produced by this technique was beyond the scope of this project but based on observation using the laser optics we estimate that the majority of U particles were between 2 and 5µm. Thus, although we attempted to select the smallest sized particles that were visible it is likely that initial testing was performed on particles that were significantly larger than the ~1µm that is relevant to work performed by the IAEA.

However, this testing was still a critical part of method development that enabled us to characterize the typical ablation plot produced by particle ablation and the best way to handle the data produced.

As U200 contains ~20% ^{235}U, the tests were performed with ^{235}U on the L5 Faraday detector. The choice of detector for ^{235}U requires some discussion. In samples with higher ^{235}U enrichments a Faraday detector is required as the ^{235}U signal is at risk of saturating an ion counter. In contrast, if a depleted uranium sample is analyzed the ^{235}U signal is likely to be too low to measure well by Faraday, resulting in large uncertainties on the final ^{235}U/^{238}U ratio. In this case an ion counter is the better choice. However, for unknown samples the degree of ^{235}U enrichment is also unknown, meaning we do not have the information required to choose the appropriate detector. Where we are performing analysis of micron-scale particles the sample will be rapidly destroyed during the ablation process, so the measurement cannot be repeated. Thus, we recommend that both ^{235}U and ^{238}U are measured by Faraday detector for safeguards purposes. In this case, we can guarantee usable ^{235}U/^{238}U data (albeit with potentially lower precision), rather than potentially saturating the ion counter and obtaining incorrect ^{235}U/^{238}U ratios.

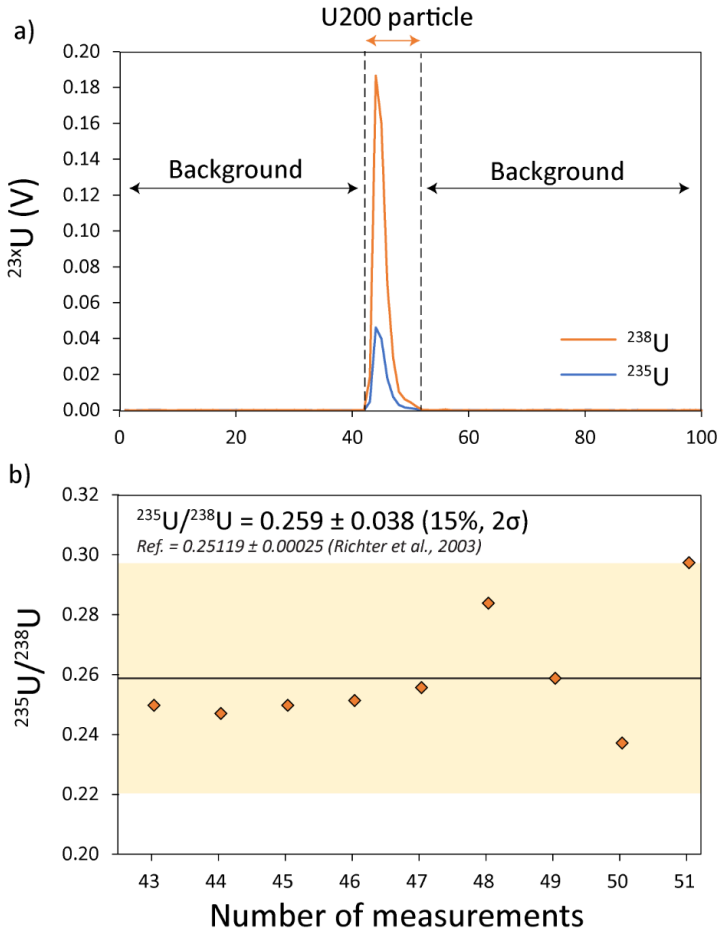

Figure 19 – a) Uranium plot generated by ablation of a single micron-scale particle of the U200 reference standard, b) isotope ratio data collected for the U200 particle.

6.4. Ablation characteristics of micron-scale uranium particles.

The plot generated from a single U200 particle is shown in Figure 19. The U signal lasts for ~10 integrations, which corresponds to <3 seconds of data. In this case, maximum ^{238}U and ^{235}U intensities were in the 10's to 100's of mV range, which were easily measurable by Faraday detector, but the signal is highly unstable compared to that generated by a glass standard (Figure 5). We initially treated the particle data similarly to how we would reduce data derived from a glass standard. The final $^{235}U/^{238}U$ ratio for a particle was calculated from all of the integrations in which ^{238}U intensities were greater than 1mV (Figure 19a and b). In the example shown in Figure 19, this yielded a final $^{235}U/^{238}U$ ratio of 0.259 ± 0.038 (2σ) (Figure 19b). Although this value is within uncertainty of the reference value of 0.25119 ± 0.00025 (Richter et al., 2003) the uncertainty associated with this isotope ratio is orders of magnitude less precise with an RSD of ~15%. The problem here is that there is a restricted amount of data and all the data points are treated equally, meaning ratios generated from low intensity integrations can have a disproportionate effect on the final result. For this reason, it may not be correct to reduce data generated from U-particles in the same way that we would reduce data from a glass or other homogenous solid material.

To address this problem, we devised a new approach to handling U isotope data obtained from particles. Instead of simply averaging the line-by-line isotope ratios for each particle, the intensities from each isotope were summed, which in effect gives more weighting to data points with higher ^{23x}U intensities. Based on the scatter in the background prior to and after the sample signal we established a threshold value of 0.3mV of ^{238}U, above which we assume we are recording the U isotope signal associated with the particle rather than fluctuations in the background. Final uranium data was summed for all integrations in which ^{238}U was >0.3mV. Uncertainties were calculated using basic counting statistical techniques and the uncertainty in the background was incorporated into this error estimation. Full explanation of how isotope ratios and associated uncertainties were calculated are provided in Section 7. Particle data obtained individually, or through rastering, were reduced identically.

Table 8 – Uranium isotope ratios for a single particle of U200. The data has been reduced by two methods; treating the data as a glass or as a particle.

	$^{235}U/^{238}U$	2s	%	$^{234}U/^{238}U$	2s	%	$^{236}U/^{238}U$	2s	%
Glass reduction	0.260	0.040	16%	0.00102	0.00076	74%	0.0017	0.0012	70%
Particle reduction	0.25018	0.00366	1.5%	0.001433	0.000018	1.2%	0.002286	0.000025	1.1%
Reference (Richter et al., 2003)	0.25119	0.00025	0.1%	0.0015661	0.0000021	0.1%	0.0026549	0.0000019	0.1%

As shown in Table 8, there are inherent differences between U-isotope data from a particle of U-200, depending on the method of reduction. The 'particle' reduction method produces data that is both more accurate and more precise than the 'glass' reduction method, with typical uncertainties of 1 to 1.5% on $^{235}U/^{238}U$, $^{234}U/^{238}U$ and $^{236}U/^{238}U$ ratios.

6.5. Characterization of NIST SRM U200 (U_3O_8 powder)

The uranium isotopic composition of 49 particles of U200 are provided in Table 9 and presented in Figure 20. On average, the $^{235}U/^{238}U$, $^{234}U/^{238}U$ and $^{236}U/^{238}U$ ratios are within uncertainty of the reference values (Richter et al., 2003). The standard deviation of the average $^{235}U/^{238}U$ ratios of the U200 population equates to an RSD of ~2.5%, which is similar to the uncertainties on the $^{235}U/^{238}U$ ratios of the individual particles. As expected, these uncertainties are over an order of magnitude higher than were generated by the U reference glasses (RSD's of 0.1-0.2%, Section 5) and the IAEA's international target values for ^{235}U abundance measurement by solution MC-ICP-MS (0.07% for HEU). The uncertainties on our new data are similar to those generated previously for U-particle analysis by laser ablation (e.g. Donard et al., 2017; Ronzini et al., 2019; Craig et al., 2020) and, as the IAEA currently has no recommended ITV for U-isotopic analysis in particles by laser ablation MC-ICP-MS, an uncertainty of ~2.5% for a $^{235}U/^{238}U$ ratio may be a more relevant benchmark to add in future ITV revisions.

Table 9 – Uranium isotope data from replicate analyses of the U200 particles. Data is provided with and without outlier rejection for the $^{234}U/^{238}U$ and $^{236}U/^{238}U$ ratios

	$^{235}U/^{238}U$	2σ	RSD (%)	$^{234}U/^{238}U$	2σ	RSD (%)	$^{236}U/^{238}U$	2σ	RSD (%)
All data (n=49)	0.2517	0.0062	2.5	0.00148	0.00050	34.0	0.00242	0.00083	34.3
Outliers excluded (n=46)	N/A	N/A	N/A	0.00152	0.00018	11.6	0.00250	0.00034	13.5
Reference value (Richter et al., 2003)	0.25119	0.00025	0.1	0.0015661	0.0000021	0.1	0.0026549	0.0000019	0.1

Over the course of these analyses, several data points were excluded based on low or negligible ^{238}U and ^{235}U counts. We assume that these were either imperfections on the planchet or dust particles that were misidentified as uranium particles. A subset of U-particles (2 out of 50) have $^{234}U/^{238}U$ and $^{236}U/^{238}U$ ratios that are resolvable outside of 2σ uncertainty from the main sample population. If these data are excluded, the reproducibility of $^{234}U/^{238}U$ and $^{236}U/^{238}U$ values in the main population is improved by a factor of ~3 (Figure 21). These anomalous U-isotope ratios either reflect heterogeneities in the U200 reference material or inconsistencies associated with the data collection or reduction protocols. In this case, we hypothesize that the former is correct. If the U-isotope ratios are plotted in 3-isotope space (Figure 22), there is a clear correlation between the $^{236}U/^{238}U$-$^{234}U/^{238}U$ ratios and a trend towards higher $^{235}U/^{238}U$ ratios with decreasing $^{236}U/^{238}U$. This indicates mixing with a contaminant that has relatively depleted ^{234}U and ^{236}U contents (Figure 22a) and relatively enriched ^{235}U (Figure 22b).

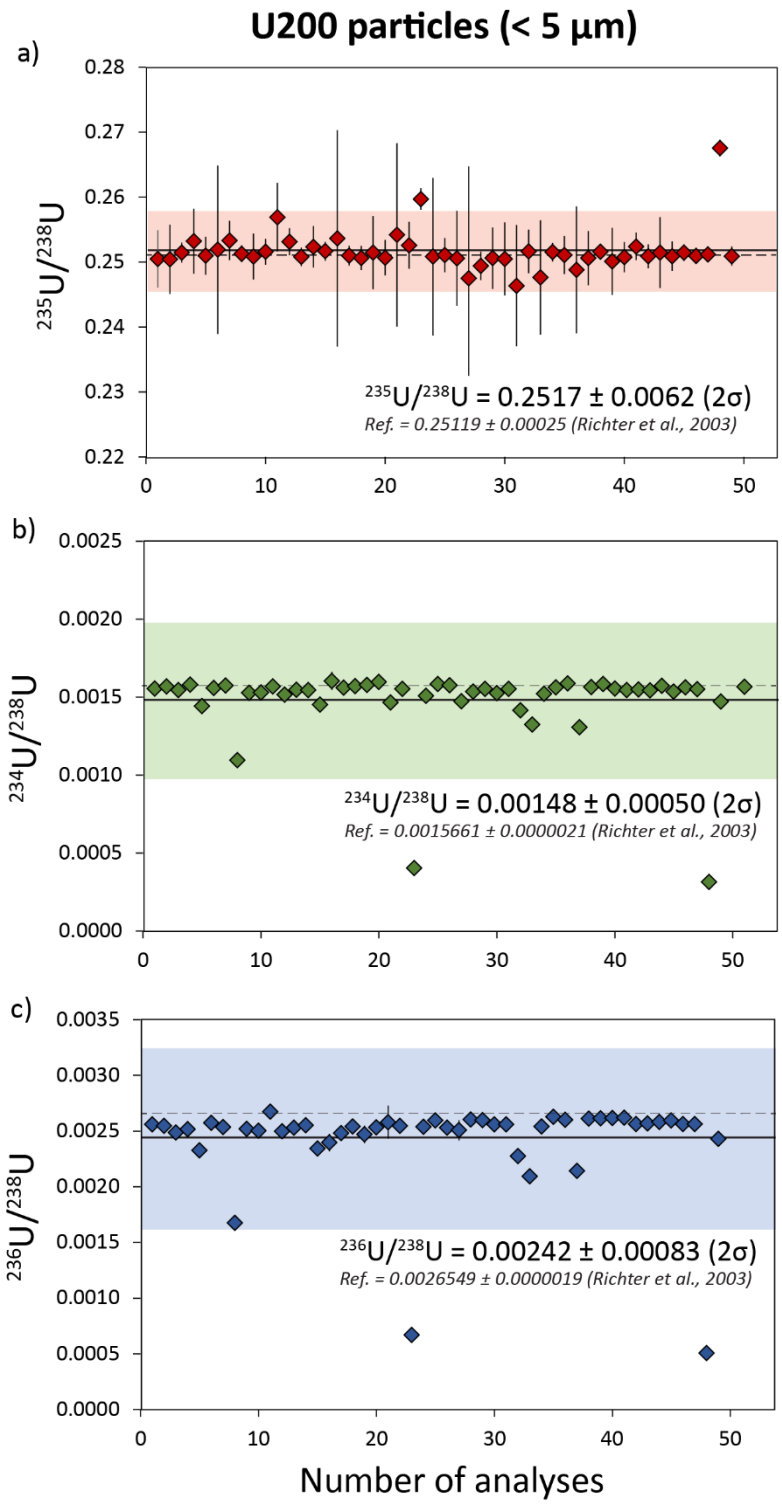

Figure 20 – Uranium isotope systematics for 49 separate U200 particles. Reference isotope ratios are taken from Richter et al., (2003). Uncertainties are 2σ.

A two-component mixing array could be generated by agglomerating particles with isotopically distinct uranium compositions. The particle sizes generated by the in-house dispersal of U200 were highly variable and generally larger than 1 micron, meaning individual particles could represent a mixture of components. In general, the contaminant phase in U200 imparts relatively minor variations to the U isotope ratios, and the heterogeneities are only observed in a subset of U-particles. This indicates that it is unlikely to be a significant source of isotopic heterogeneity at the bulk level. However, this neatly illustrates the effectiveness of characterizing U-isotope ratios at the particle scale by laser ablation MC-ICP-MS and the potential for identifying isotopic signatures that may not be apparent using bulk dissolution techniques.

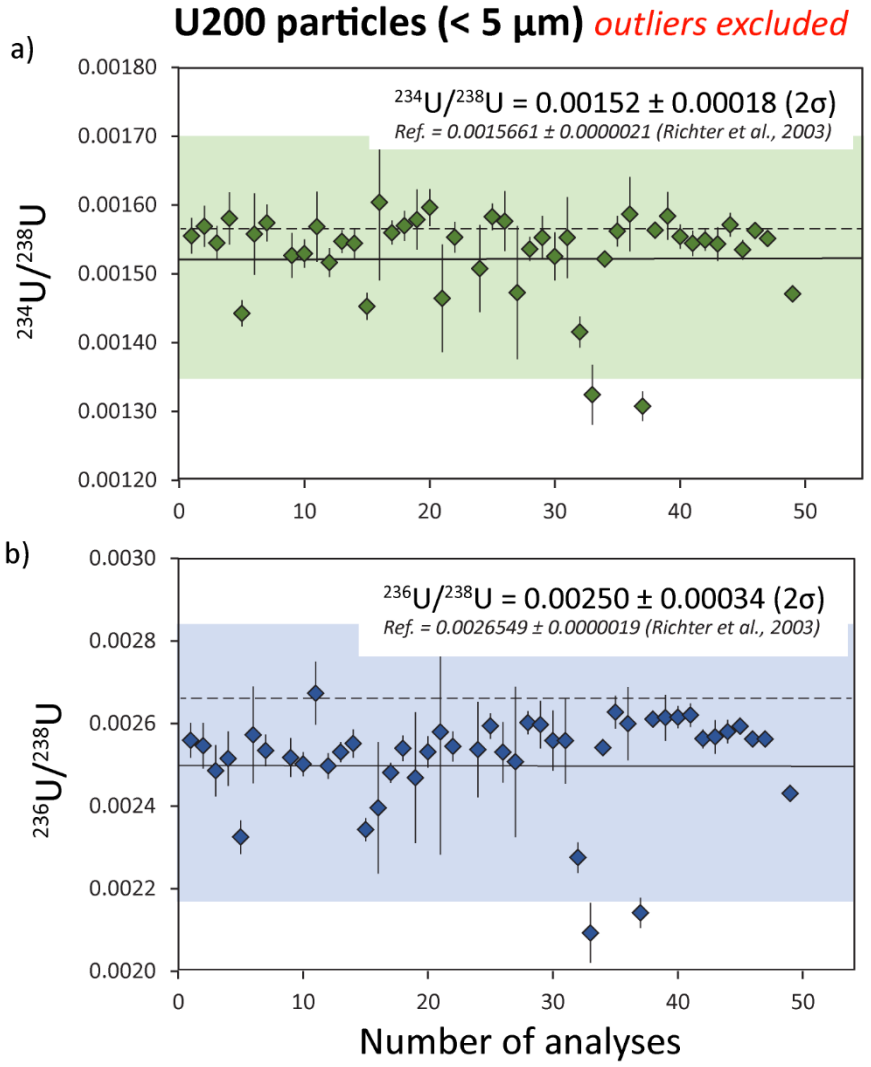

Figure 21 – Minor uranium isotope ratios measured in 47 particles of the U200 reference material. Two samples with $^{234}U/^{238}U$ and $^{236}U/^{238}U$ ratios that fall outside of uncertainty of the mean (2σ) were excluded. Reference isotope ratios are taken from Richter et al., (2003). Uncertainties are 2σ.

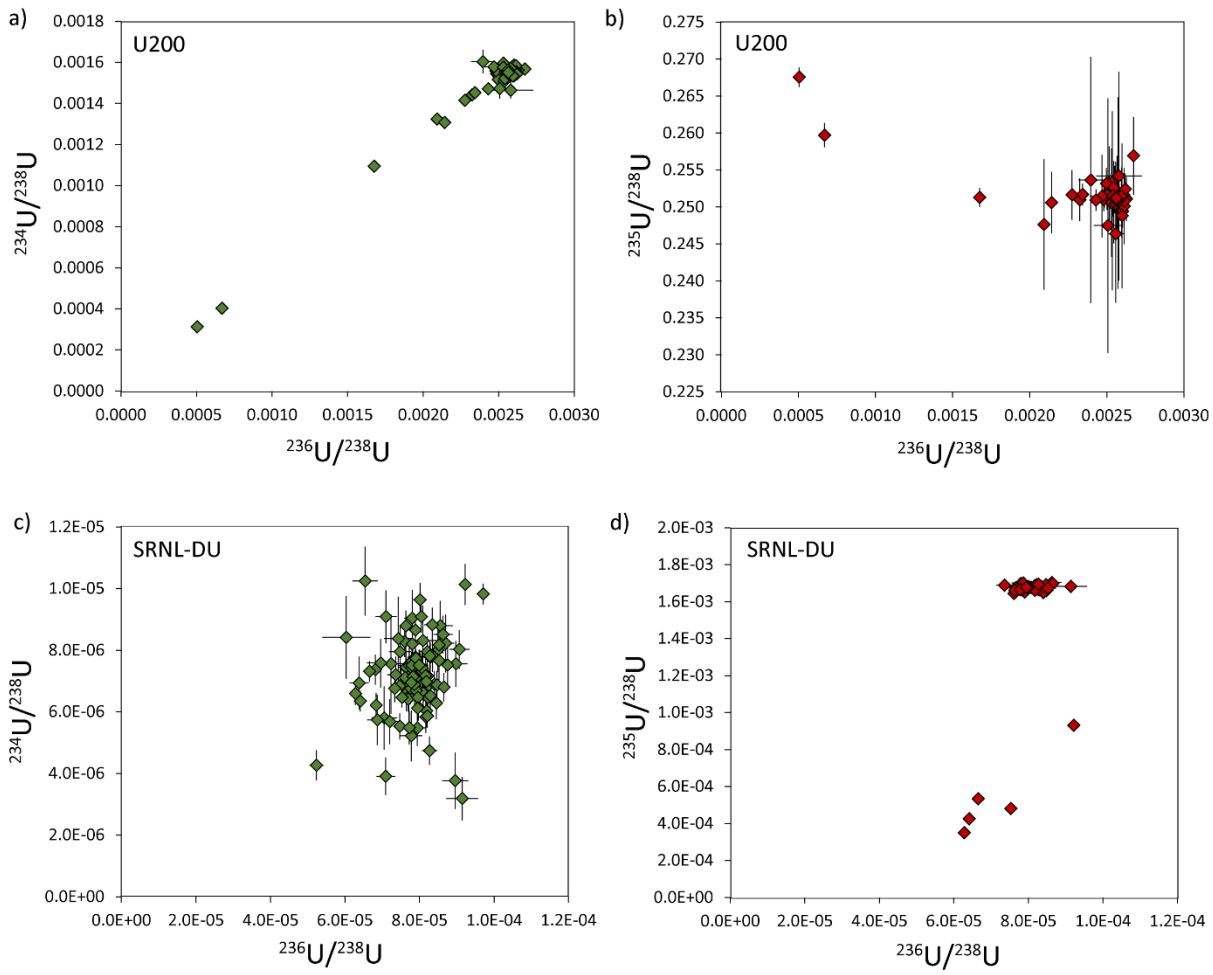

Figure 22 – Three-isotope plots of the uranium composition in U200 and SRNL-DU particles. All uncertainties are 2σ.

6.6. Characterization of SRNL-DU (Depleted Uranium)

The depleted uranium particles obtained from SRNL are composed of U_3O_8 that was produced purposely for in-situ isotopic analysis. The particles have well characterized sizes (~1 micron) and densities (~8.3 g/cc) and a total of 10^3-10^5 particles were deposited on each silicon and carbon planchet for isotopic analysis. We analyzed 103 SRNL-DU particles, with a roughly even split between those analyzed with ^{235}U on the L5 Faraday and those analyzed with ^{235}U on IC2. The results of these analyses are summarized in Table 10 and displayed in Figures 23 and 24.

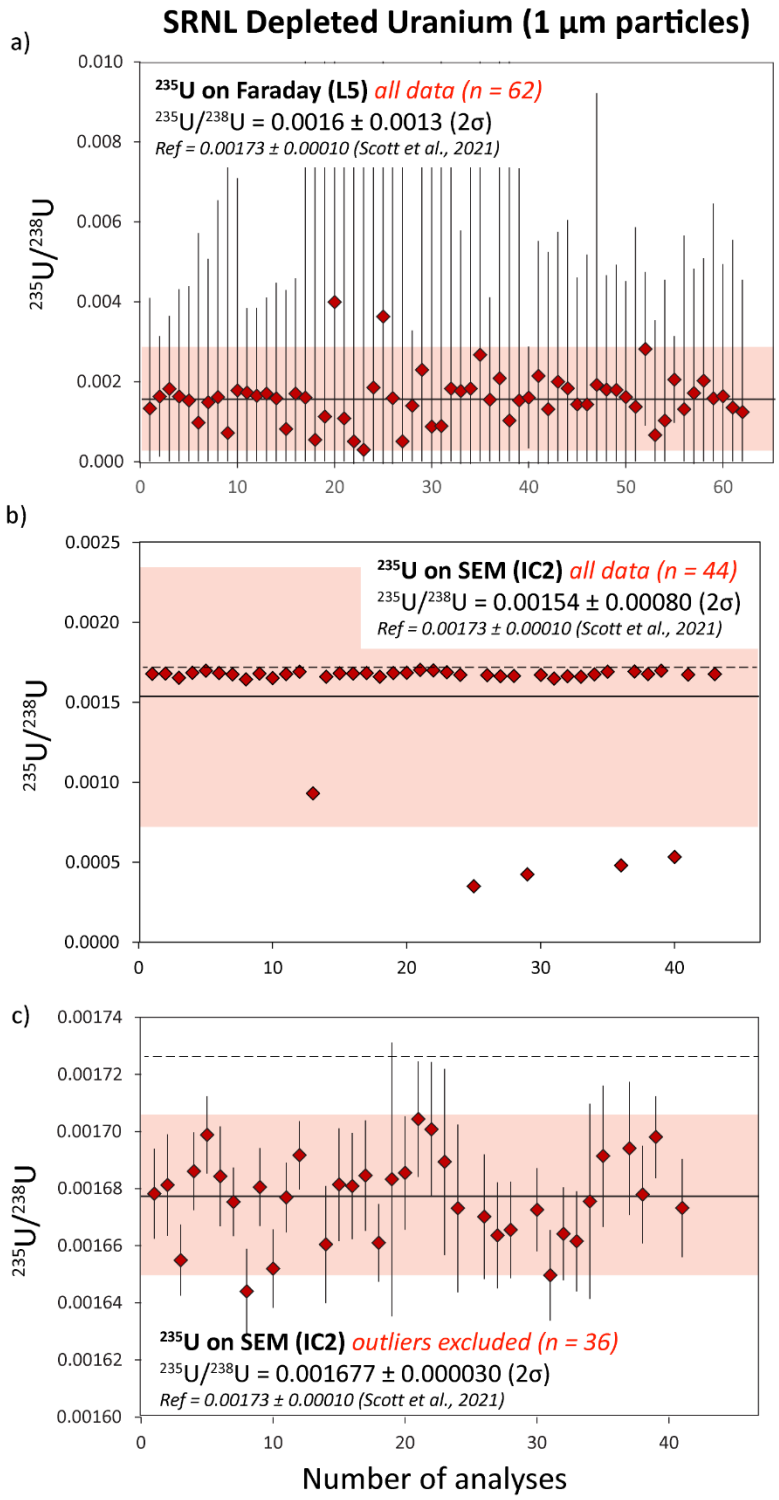

Figure 23 – $^{235}U/^{238}U$ ratios measured in SRNL-DU particles. In a) the ^{235}U was analyzed using the L5 Faraday. In b) the ^{235}U content was measured using IC2, and the final $^{235}U/^{238}U$ average with five outliers excluded are in c). All uncertainties are 2σ.

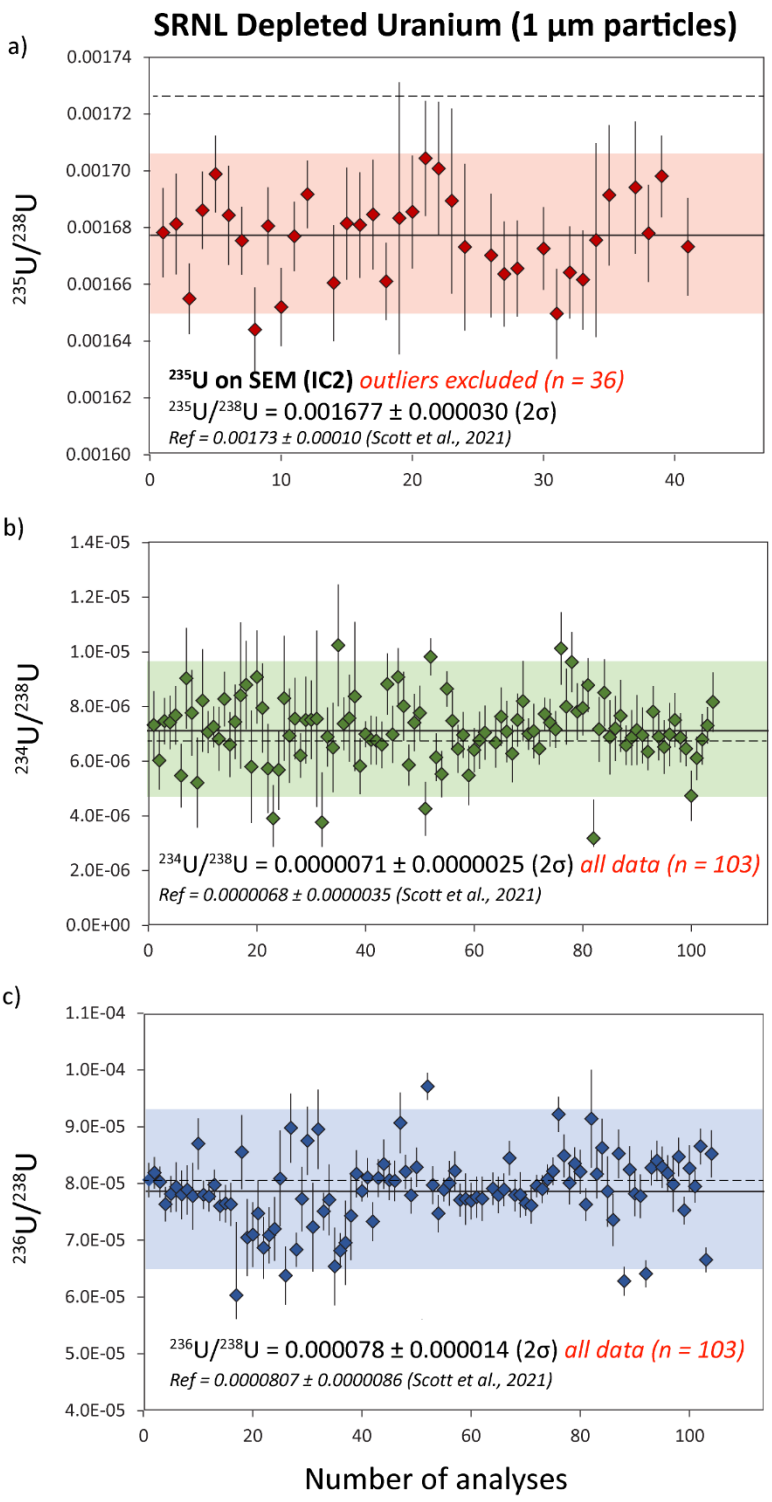

Figure 24 – Uranium isotope data from replicate analyses of SRNL-DU particles. All uncertainties are 2σ. Outlier rejection on $^{235}U/^{238}U$ based on 2σ of the mean. Samples with outlying $^{235}U/^{238}U$ ratios did not have outlying $^{234}U/^{238}U$ and $^{236}U/^{238}U$ ratios.

The SRNL-DU sample has a ^{235}U content of 0.1720 ± 0.0104%, meaning the ^{235}U content is highly depleted compared to either natural uranium or U200. Typical ^{235}U signals on the L5 Faraday were 3-4 mV, which is difficult to resolve from the background noise on the detector. As a consequence, the final $^{235}U/^{238}U$ ratios measured using this detector have large error bars, equating to RSDs of 50-200%. Although highly imprecise, these data are still broadly consistent with the highly depleted ^{235}U content of SRNL-DU. On average, we obtained a $^{235}U/^{238}U$ ratio of 0.0016 ± 0.0013 (2σ) from 62 measurements of SRNL-DU measured with ^{235}U on the L5 Faraday (Figure 23a), which is consistent with the reference value (Table 10).

As would be expected, the $^{235}U/^{238}U$ ratios generated with ^{235}U on IC2 were far more precise. In this case, typical ^{235}U counts on IC2 were ~10-12k cps, which were easily measurable above background levels (<5 cps). Uncertainties on $^{235}U/^{238}U$ ratios of individual particles were typically <2%. If all data were included, we obtained a final average $^{235}U/^{238}U$ ratio of 0.00154 ± 0.00080 (2σ), as shown in Figure 23b. The large RSD (53%) is driven by a subset of samples with relatively depleted ^{235}U contents, that fall outside of the 2σ uncertainty associated with the mean (Figure 22d). If these samples are excluded, the average $^{235}U/^{238}U$ value of the main population can be more precisely defined, with a value of 0.001677 ± 0.000030 (2σ), which equates to an RSD of 1.8% (Figure 23c). This is within uncertainty of the reference value obtained by LG-SIMS (Scott et al., 2021), as presented in Table 10.

Table 10 – Uranium isotope data for the SRNL-DU particle sample obtained by laser ablation. Data for $^{234}U/^{238}U$ and $^{236}U/^{238}U$ derive from 103 separate analyses. Data for $^{235}U/^{238}U$ with ^{235}U on IC2 derive from 36 measurements, whereas data with ^{235}U on L5 derive from 62 measurements. Uncertainties are 2σ. *Reference values from LG-SIMS analyses are provided from Scott et al., (2021).

Isotopic composition	**$^{234}U/^{238}U$**	**2σ**	**$^{235}U/^{238}U$**	**2σ**	**$^{236}U/^{238}U$**	**2σ**
Laser Ablation (^{235}U IC2)	0.0000071	0.0000025	0.001677	0.000030	0.000078	0.000014
Laser Ablation (^{235}U L5)			0.0016	0.0013		
LG-SIMS (single particle)*	0.0000068	0.0000035	0.00173	0.00010	0.0000807	0.0000086
LG-SIMS (particle mapping)*	0.0000088		0.00174		0.000079	
Isotopic distribution	**^{234}U**	**^{235}U**	**^{236}U**	**^{238}U**		
Laser Ablation (LLNL)	0.00071%	0.1674%	0.0078%	99.82%		
LG-SIMS*	0.00068%	0.1720%	0.00804%	99.640%		

The cause of the anomalous $^{235}U/^{238}U$ ratios is difficult to constrain. Unlike U200, where isotopic heterogeneities in ^{234}U, ^{235}U and ^{236}U covary (Figure 22a, b), the heterogeneities in SRNL-DU are only evident in the $^{235}U/^{238}U$ ratio (Figure 22c, d). The five DU particles with low $^{235}U/^{238}U$ ratios (<0.001) have similar $^{234}U/^{238}U$ and $^{236}U/^{238}U$ ratios to the rest of the sample population, indicating that their anomalously low $^{235}U/^{238}U$ ratios derive from relative depletions in ^{235}U, rather than simple addition of ^{238}U. Although anomalous $^{235}U/^{238}U$ values could be analytical in origin, there

is no logical reason why samples with relatively elevated ^{238}U intensities should have relatively suppressed ^{235}U signals. The maximum ^{235}U intensities for SRNL-DU were between 10-20 kcps, far too low to have been affected by detector dead time. For example, we were able to obtain accurate $^{235}U/^{238}U$ ratios for CAS-500-Nat glass with ^{235}U intensities >100 kcps, an order of magnitude higher than ^{235}U intensities from SRNL-DU particles (see Section 5). Peak tailing effects from a high ^{238}U beam are also unlikely to explain the data; in this case we would expect peak tailing to be more prominent on the $^{236}U/^{238}U$ ratio, which is not the case. Alternatively, these data could reflect some minor ^{235}U heterogeneity within the deposited U_3O_8 particle population. In theory, a subset of the SRNL-DU particles with slightly larger grain sizes and lower $^{235}U/^{238}U$ ratios could have been deposited alongside the main sample population. This would need to be verified using better imaging techniques and/or secondary ion mass spectrometry (SIMS). Current analysis of SRNL-DU by LG-SIMS has not identified a contaminant phase (Scott et al., 2021).

The broadscale homogeneity of $^{234}U/^{238}U$ and $^{236}U/^{238}U$ ratios throughout the SRNL-DU population enabled more straightforward characterization of the minor isotope abundances (Figure 24). From 103 measurements of SRNL-DU we obtained an average $^{234}U/^{238}U$ ratio of 0.0000071 ± 0.0000025 (2σ) and average $^{236}U/^{238}U$ ratio of 0.000078 ± 0.000014 (2σ). These values are within uncertainty of the LG-SIMS data (Table 10), meaning there is close agreement between the final isotopic distribution for SRNL-DU obtained by LG-SIMS and laser-ablation MC-ICP-MS.

6.7. Conclusion: characterizing U-isotope systematics in particles by laser ablation MC-IC-MS

Our testing demonstrated that laser ablation MC-ICP-MS is a fast and reliable technique to obtain U isotope data in U-particles. Based on testing with NIST SRM U200, we estimate that a maximum precision of 1.5-2% can be obtained for the $^{235}U/^{238}U$ ratio in samples with >10-20% ^{235}U. Similar precision can also be obtained for low-enriched, natural and depleted uranium samples, such as SRNL-DU, if ^{235}U can be measured by ion-counter. Using this method, we obtained $^{235}U/^{238}U$ ratios for SRNL-DU that were within uncertainty of values obtained by LG-SIMS, with comparable uncertainty. In mission relevant scenarios, where the ^{235}U enrichment level is not known, it is possible that an unknown sample will have a high enough ^{235}U enrichment factor that the ^{235}U signal saturates the ion counter. In this case the $^{235}U/^{238}U$ data would not be usable. Thus, we recommend that both ^{235}U and ^{238}U be measured by Faraday detector on unknowns, unless some bounding limits on the enrichment factor exists. Although the precision of Faraday analysis suffers in depleted uranium samples (~80%), it is clear that the technique is still sensitive enough to distinguish between samples of different enrichment levels. We also show that laser ablation MC-ICP-MS can be used to obtain accurate minor isotope data (^{234}U, ^{236}U) from U-particles. The $^{234}U/^{238}U$ and $^{236}U/^{238}U$ ratios obtained for SRNL-DU are fully consistent with reference values obtained by LG-SIMS. Using laser ablation MC-ICP-MS we are able to resolve ^{234}U contents of <10ppm and ^{236}U contents <80ppm in micron scale particles of depleted uranium. This indicates that laser ablation MC-ICP-MS is a viable technique to characterize the isotopic composition of U-particles for IAEA safeguards.

To further develop this technique would require testing with mission relevant samples, i.e. with unknown or mixed isotopic compositions. It is also unclear how different laser systems (e.g. femtosecond lasers) or mass spectrometers (e.g. single collector ICP-MS) would perform. For example, it is possible that multi-collector ICP-MS instruments do not provide a huge advantage over single-collectors when dealing with a highly transient signal.

The analysis of particles on swipe samples is the ultimate challenge for this technique. Dealing with particles deposited on a flat surface (as we do here) is very different to that where the substrate has significant vertical relief (such as a swipe). The laser system is fine tuned to focus on the sample surface, meaning flat samples can easily be navigated without refocusing the optics. The challenge with swipes is that the surface is not flat and hence particles would occupy different depths within the substrate, meaning an automated raster may miss, or incompletely ablate, a high % of particles present. Developing methodology to deal with swipe samples would be the logical next step in advancing this capability.

7. Development of the Laser Ablation Reduction Application (LARA)

7.1. The brief: develop a computer application to reduce laser ablation data

The LARA reduction script is designed to handle U-isotope data obtained by laser ablation MC-ICP-MS. This analytical method generates a large amount of data that is unwieldy to reduce by hand and cannot easily be reduced using online software. Although reduction programs for laser ablation ICP-MS exist (e.g. Iolite, Glitter), they are not optimized for U-isotope measurements and, in particular, have not been designed for analysis of micron-scale particles in which the generated signal is highly transient; lasting for just a few seconds. Furthermore, it is unclear how these ‘black box’ systems handle the various sources of uncertainties associated with the measurement and correction for mass bias. For these reasons, the creation of a tailored reduction program designed specifically to handle particle data was a key component of this project.

The reducer was written in R-script but we recognize that many users are unfamiliar with this (or any) programming language. Therefore, the decision was made to create a user friendly ‘app’ using the Shiny package that operates in the R environment. The LARA interface is designed to be used by the non-expert and we have attempted to include as much functionality and flexibility as possible, enabling data to be exported in Excel readable files and a variety of figures to be generated. LARA is able to handle U-isotope data obtained from glasses and/or solid samples in which depth profiling is undertaken, or particles in which the entire sample is consumed in a few pulses. It can also handle individual particle analysis or longer rastering runs of the laser over a wider area.

7.2. Summary of code functionality

The LARA reducer accesses raw, time-resolved isotope signal intensities output by the Neptune MC-ICP-MS software and the full dataset (e.g. 200 lines of data for a glass standard) is exported as an Excel readable .exp file. Raw data for ^{233}U, ^{234}U, ^{235}U, ^{236}U and ^{238}U is obtained for each individual analysis and sequence are comprised of analyses of samples and reference standards. The isotopic data from these reference standards are used by LARA to calculate parameters such as mass bias and ion-counter gain, which are used to automatically correct data from the unknowns.

In brief, LARA must follow a set procedure to process the raw intensities from each sequence and obtain corrected isotope ratios for each unknown:

1. Identify which data are from standards and which are from unknowns.
2. For each sample and standard identify the portion of the plot that is derived from the gas blank, and the portion of the plot in which ablation of the sample takes place (see figure 25).
3. Calculate raw isotope ratios for each sample and standard. The method will differ depending on whether the samples are glasses or particles.
4. Subtract the background intensities from each sample and standard.
5. Calculate the mass bias factors during the analytical sequence. This is calculated by comparing the measured $^{235}U/^{238}U$ ratio of a standard with the reference value. The proportional difference between measured and known can be used to correct U isotope ratios in the unknowns. The mass bias may shift during the sequence; therefore, multiple mass bias standards are measured throughout the sequence and an interpolated correction factor is applied.
6. Calculate ion counter gain factors for ^{233}U, ^{234}U and ^{236}U. This is required because the ^{238}U and ^{235}U intensities are typically measured by Faraday detector, which are pre-calibrated to each other but not to the various ion counters. This correction factor is generated by comparing the measured IC/Faraday ratio (e.g. $^{234}U/^{238}U$) after mass bias correction to the known ratio. This correction factor is also interpolated based on repeat measurements of the reference standard. Where online ion counter gains cannot be calculated there is also the option of applying a user-defined IC gain constant.
7. Uncertainties associated with the measurement of each unknown is combined with uncertainty related to the mass bias/gain corrections. The uncertainty of the known ratios for the reference standard are also propagated into the final combined standard uncertainty (CSU).
8. Corrected data is exported into a .csv file and the reducer generates figures that can be edited and exported.

7.3. Detailed description of reduction protocols

7.3.1. Identification of standards and samples

Each analytical sequence is comprised of one or more sequences, in which unknowns are bracketed by reference standards that are used to correct mass bias and ion counter gains. The structure is shown below:

Reference standard (e.g. NIST 610, CAS-53_500)

Unknown

…

…

Reference standard

LARA recognizes certain standard names (e.g. CAS-53) and will identify the reference standards assuming the correct name is used during data collection. The interface will populate the U isotopic compositions of standards that are incorporated into LARA. If reference standards are used other than those entered in the reducer, or if the correct name of each standard is not used (e.g. writing C-53 rather than CAS-53) the user must populate the U isotope ratios of the reference standard by hand. If the U isotope ratios of the reference standards are not entered the reducer will pop-up an error message.

Any isotopic analysis that is not identified as the reference standard will be assumed to be an unknown and treated as such. The reducer cannot identify the difference between an unknown glass/solid sample or an unknown particle. This must be distinguished by the user in the reducer and is an important factor because these types of data are treated very differently. At present, LARA can only reduce unknowns of one sort at a time (particle or glass). Mixed runs of particles and glass standards cannot yet be reduced together.

7.3.2. Reduction of glass data

The ablation of glasses and other solid materials with homogenous compositions follows a set pattern. There is an initial period of ‘no ablation’ lasting ~20s, which is used to quantify the gas blank (Figure 25a). This is followed by the ablation period. Here, the initial 2-3 seconds of ablation is relatively unstable as the analyte is transferred to the plasma source of the mass spectrometer marked by an initial steep increase of signal. This is followed by a relatively stable period of steadily decreasing signal, which generally lasts for 30-40s and has the least variable isotope ratios. This stable region of the ablation plot is selected for by LARA. A simple logical screening routine was added to identify the pulse cycle index of maximum ^{238}U intensity, which unequivocally corresponded to the beginning of “on-peak” U measurement shortly after initiating the ablation process. All data from this cycle to the completion of the analysis routine was used to calculate ^{238}U-normalized uranium isotope ratios and corresponding uncertainties (standard deviation and standard error).

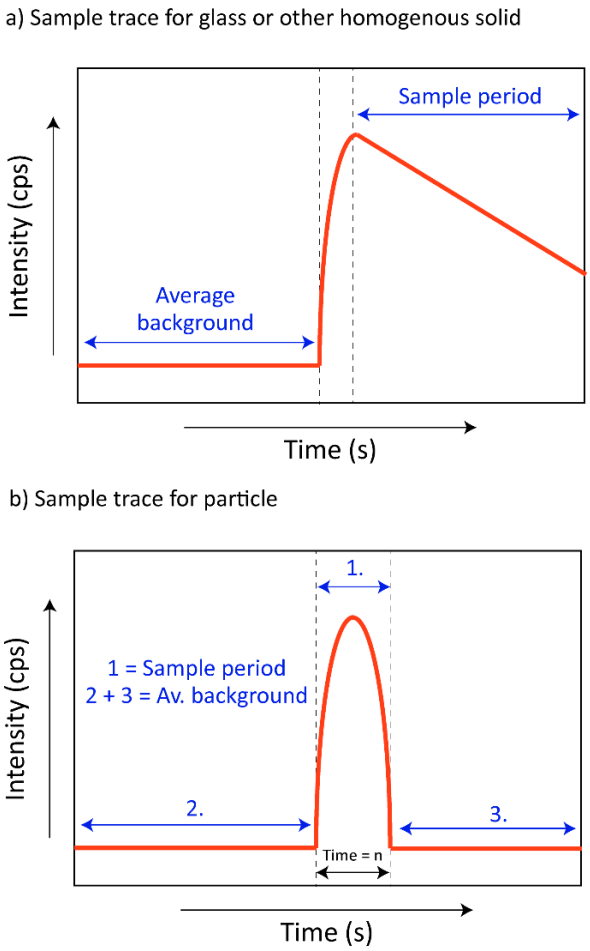

Figure 25 – Schematic of the data generated by a) glass/solid sample and b) a U-particle.

7.3.3. Reduction of particle data

During the analysis of uranium particles the ablation period is very short (2-3s) the data generated from each particle accrues for a short period of time and must be handled differently to data derived from a glass or solid sample. As described in Section 6, we sum all of the data collected above a threshold of 0.3mV of ^{238}U. The ablation plot is then split into regions of background (Regions 2 and 3 in Figure 25) and sample (Region 1 in Figure 25) and the data reduction and uncertainty calculation follows the procedure below:

The procedure to reduce single or multiple particles is the same and is described below:

i. Sample intensities/voltages in Region-1 (Figure 25) are summed for each particle.
ii. Faraday signals are converted into intensities (cps) assuming that 1mV = 62415 counts per second.
iii. Uncertainties associated with the sample signal are calculated assuming a normal distribution and using standard counting statistical techniques as shown in Equation 1,

where $\Sigma^{23x}U_{sample}$ refers to the number of counts of isotope ^{23x}U from each particle (Region-1, Figure 25), where x represents ^{234}U, ^{235}U, ^{236}U or ^{238}U.

$$Std.Uncert.{}^{23x}U_{sample} = \sqrt{\sum {}^{23x}U_{sample}} \qquad \textit{Equation 1}$$

iv. However, this simple calculation underestimates error, because it doesn't take into account the noise from the detector. This is particularly important for isotopes measured by Faraday detector as mV signals are converted to count rates of 10's-100's kcps, which generate very low uncertainties based purely on Equation-1. Actually, mV-level signals are close to the detection limits of Faraday detectors, meaning the instability in background signal adds a significant uncertainty to the final sample analysis that must be incorporated. This background is calculated in equation 2, where $\sigma^{23x}U$ is the standard deviation of the background for isotope ^{23x}U (in cps), and $N^{23x}U_{sample}$ is the number of data points in Region-1 (Figure 25) from which the background counts are summed.

$$\sum {}^{23x}U_{background} = \sigma^{23x}U_{background} \times N^{23x}U_{sample} \qquad \textit{Equation 2}$$

v. The sample and background uncertainties are then summed to obtain a final measurement uncertainty for each isotope:

$$Std.Uncert.{}^{23x}U_{Total} = Std.Uncert.{}^{23x}U_{sample} + \sum {}^{23x}U_{background} \qquad \textit{Equation 3}$$

vi. The final uncertainties for each ratio are then calculated using Equation 4:

$$Std.Uncert.\left(\frac{{}^{23x}U}{{}^{238}U}\right) = \frac{\sum {}^{23x}U}{\sum {}^{238}U} \times \sqrt{\left(\frac{Std.Uncert.{}^{23x}U_{Total}}{\sum {}^{23x}U}\right)^2 + \left(\frac{Std.Uncert.{}^{238}U_{Total}}{\sum {}^{238}U}\right)^2} \qquad \textit{Equation 4}$$

In addition to the ablation of single particles, the system can also raster over a wider area and potentially collect sample data from numerous individual particles without prior identification (Figures 18 and 26). Due to the convenience of this technique, LARA can also reduce multiple particles from a single .exp file. Although this was designed to support the ability to raster over an area, in theory this option could also reduce any file that contains data from multiple samples (e.g. a long line scan or manual ablation over a wide area).

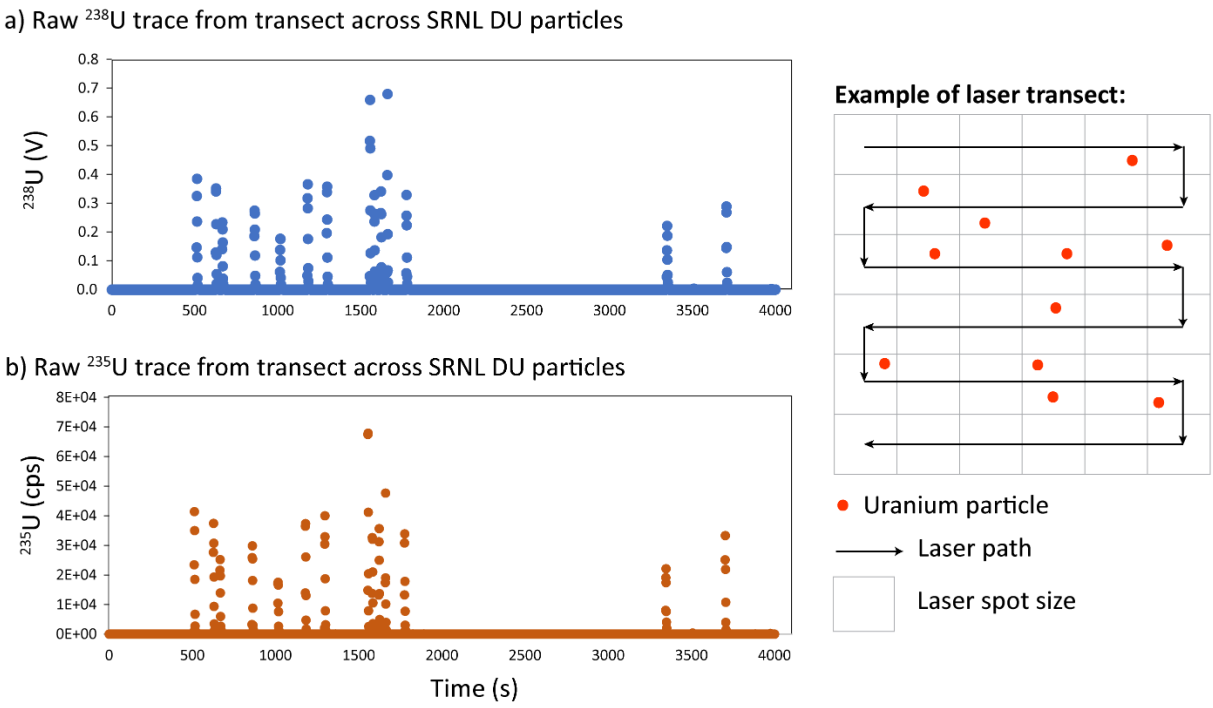

Figure 26 – Uranium data from a transect across a silicon planchet containing SRNL-DU. As shown, multiple U-particles were ablated over the ~1 hour ablation period.

7.4. Corrections applied to final uranium isotope data

7.4.1. Mass bias

Raw isotope ratios determined by mass spectrometry are inaccurate, due to mass bias effects that favor the transmission of heavy isotopes through the mass spectrometer. Hence a measured $^{235}U/^{238}U$ ratio will be smaller than the true ratio as ^{238}U is preferentially transmitted during the analysis. To correct for these effects the isotopic composition of a mass bias standard is measured alongside the unknowns and a mass bias factor is calculated based on the proportional difference between the measured and known isotope ratio. In this project we have used the CAS-53-500 glass standard to correct mass bias and gains. The advantage of this material is that it contains ~50% ^{235}U meaning both ^{235}U and ^{238}U can be measured on Faraday detectors, rather than a mixed detector setup which would increase the associated uncertainty. That being said, any reference material that is relatively isotopically homogenous and has a well characterized isotopic composition could be used for mass bias correction purposes. Calculation of the mass bias factor (MBF) is performed using Equation 5:

$$MBF = \frac{ln\left[\frac{\left(^{235}U/^{238}U\right)_{STD\_measured}}{\left(^{235}U/^{238}U\right)_{STD\_true}}\right]}{ln\left[M^{235}U/M^{238}U\right]} \qquad \textit{Equation 5}$$

Where the measured and true isotope ratios are those of a reference standard and M is the mass of the isotope.

The MBF can then be used to correct the isotopic composition of an unknown using Equation 6:

$$\frac{^{235}U}{^{238}U}_{SMP\_unknown} = \frac{^{235}U}{^{238}U}_{SMP\_measured} \times \left(M^{^{235}U}/M^{^{238}U}\right)^{MBF} \qquad \textit{Equation 6}$$

The MBF is not a constant value throughout each analytical sequence. Drift is common and typically follows a systematic shift towards smaller or larger values, depending on the daily run parameters. For this reason, it is beneficial to measure the mass bias standard multiple times throughout an analytical sequence in order to characterize temporal changes in the MBF and apply an interpolated correction to the unknowns, as illustrated in Figure 27. This is a linear correction between mass bias standards with a conservative expansion of uncertainty for terms applied to unknowns to account for potential non-linear drift. Final errors associated with corrected isotope ratios include all relevant sources of measurement and instrument calibration uncertainty, which were propagated into the reported and plotted U isotope ratios via the Monte Carlo method.

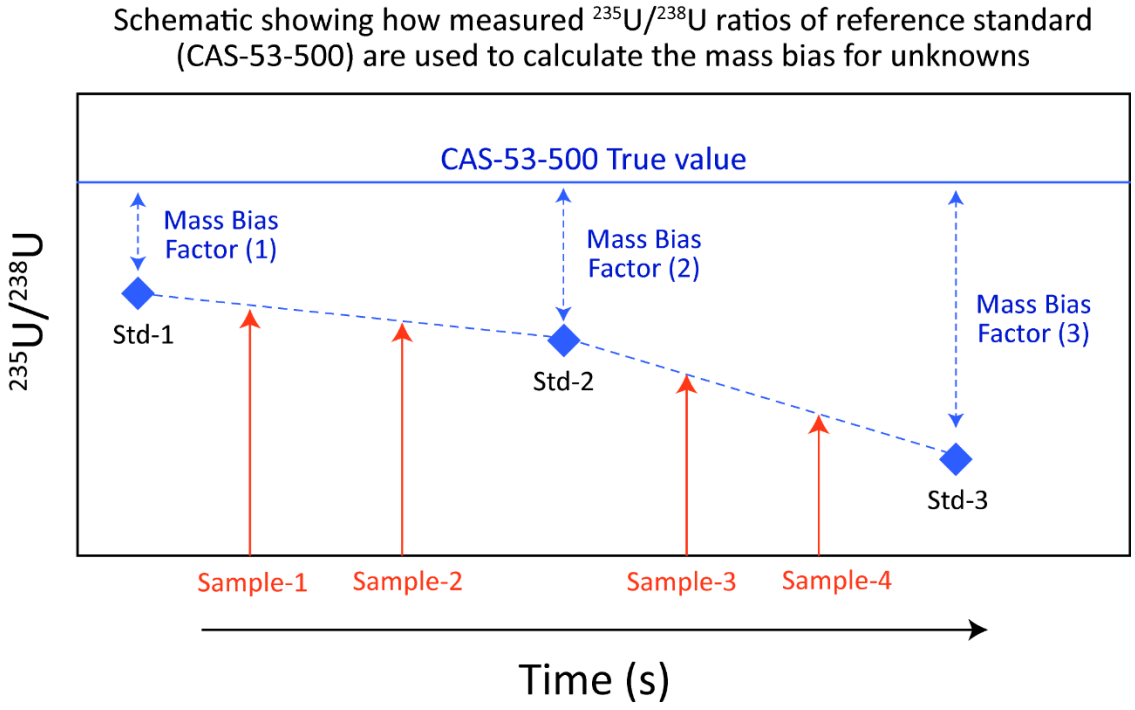

Figure 27 – Schematic illustrating drift in the mass bias over time. Samples are analyzed in between two mass bias standards and the estimated mass bias factor for each unknown is calculated by interpolating the mass bias factor between standards.

7.4.2. Ion counter gain

Signals measured by secondary electron multiplier (SEM) or compact discreet dynode (CDD) are generated by pulse counting, giving final intensities as counts per second or cps. These types of detector are often called 'ion counters' and are used for low-level signals. In contrast, Faraday detectors are used for much larger signals where the ion beam generates a current that is converted to a voltage, which is then recorded by the mass spectrometer. Faraday efficiency is calibrated online by the instrument software, ensuring that the signal generated on one Faraday is the same as another. However, there is no easy way to cross calibrate between signals recorded by both Faraday detectors and ion counters. A rule of thumb is that a 1mV signal on a Faraday detector is equivalent to 62415 cps on an ion counter. However, ion counters have a relatively short lifespan and their performance degrades over time, resulting in a decrease in the signal intensity generated by an analyte of given concentration. This means that each individual ion counter behaves differently, and a separate correction (or gain factor) must be applied to the measured signals.

The default setup for the reducer is to use the same standard reference material (in this case CAS-53-500) to calculate both the mass-bias and ion counter gains. This applies to three minor isotopes of uranium; ^{233}U (IC5), ^{234}U (IC3) and ^{236}U (IC1B) which are ratioed to ^{238}U. Once the MBF has been calculated from the CAS-53-500 standard using Equation 5, it can be used to calculate the corrected ^{233}U/^{238}U, ^{234}U/^{238}U and ^{236}U/^{238}U ratios for the same standard. This just requires a simple modification to Equation 6, as shown below in Equation 7:

$$\left(\frac{^{23x}U}{^{238}U}\right)_{SMP\_unknown} = \left(\frac{^{23x}U}{^{238}U}\right)_{SMP\_measured} \times \left(M^{^{23x}U}/M^{^{238}U}\right)^{MBF} \qquad \textit{Equation 7}$$

Where ^{23x}U refers to the minor isotope measured by ion counter.

Once the corrected ^{23x}U/^{238}U ratio has been calculated for CAS-53-500 we can make a straightforward comparison between the corrected ratio and the known ratio. The difference between these values is the ion counter gain, as shown below in Equation 8 for IC3 (^{234}U):

$$IC3\ gain\ factor = \left(\frac{^{234}U}{^{238}U}_{STD\_corrected} \Big/ \frac{^{234}U}{^{238}U}_{STD\_true}\right) \qquad \textit{Equation 8}$$

Similar to the shifts in mass bias over time, we also see shifts in the ion counter gain factors during an analytical sequence. For this reason, the ion counter gain corrections are also interpolated for the unknowns, similar to the method illustrated in Figure 27 for mass bias.

One complication to the 'online' ion counter gain correction is if we want to measure ^{235}U by ion counter. In this case, the mass bias standard cannot be used as the ^{235}U is measured by Faraday detector. To address this, we analyzed low-level uranium by solution MC-ICP-MS with ^{235}U on IC2. The calculated IC2 gain factor is then integrated into the reduction script in R. We recognize that this is not an ideal solution and will introduce more scatter into the final data than an online approach. Also, this gain factor may shift significantly in between analytical sequences, particularly if these sequences take place weeks or months apart. To address this, 'offline' IC gain factors can be manually entered into the reducer and used in place of 'online' correction factors if required.

7.5. Key functionality in LARA

LARA is designed to be as user friendly as possible. Provided the user can install the base R code and run R Studio it should be straightforward to view and reduce U isotope data obtained using the Neptune MC-ICP-MS. There are several notable features built into the reducer to ensure as much functionality and flexibility as possible to the end user, including the following:

7.5.1. Choice of mass bias standards

We have included U isotope data for four of the in-house U glass standards, NIST-610 and the USGS standard GSD-1. This means that any of these reference materials can be used for correction of mass bias and ion counter gains. We recognize that the IAEA and other analytical facilities may not have access to these reference standards. Furthermore, depending on the application, it may be beneficial to utilize different standards with different U isotope ratios to correct for mass bias or for quality control testing. For this reason, we have included the option for the user to add U isotope information for their standard of choice.

7.5.2. Exclusion of individual standard and sample analysis

Once a reference standard is identified, LARA uses all individual analysis of that standard to perform the interpolated mass bias and ion counter gain corrections. This can be problematic if one or more of the reference standards produces anomalous isotopic data, for example if the wrong standard is analyzed or a technical issue arises during the ablation process. To avoid this problem, the user can navigate through the raw data plots for each standard and choose to exclude any problematic standard analysis, prior to running the reducer.

Anomalous sample data can also be problematic, particularly when plotting finalized data and calculating average isotopic compositions. For this reason the user can choose to exclude any anomalous sample data points after the reducer has run, causing any plots that were generated and calculations of the average composition (with uncertainty) to automatically be updated.

7.5.3. Choice of ion counter gain factors

LARA can be setup to perform online ion counter gain corrections or to use manually input IC gain factors. If manually input IC gain factors are required the user can edit the pre-existing value in the constants table. Note – any edits to the constants table are only saved for the current sequence of LARA. This includes edits to the reference standards and mV to counting conversion factor.

7.5.4. Interactive plotting

The plots generated by LARA are interactive, meaning that the user can select/exclude plots of interest, zoom in and out, delete data points and export edited figures. Changes made to figures

will not be recorded in the exported .csv files, meaning that any data points excluded from the plots will still be saved.

7.6. Step-by-step guide to reduction using LARA

To use LARA we recommend download and installation of the latest versions of the R-code (currently 4.1.1.) and latest version of the RStudio software, which can be found at https://www.rstudio.com/products/rstudio. A latest version of the base R-code is particularly important to ensure that the required packages can be loaded and the reducer functions correctly. Once these have been installed, the LARA app files (*app.R* and *helpers.R*) should be copied into the RStudio directory, along with data folders. In the following we provide a step-by-step guide detailing how to use LARA to reduce U isotope data produced by laser ablation MC-ICP-MS:

i) Open the RStudio program.

ii) The files pane is, by default, located in the bottom right corner of the window (Figure 28). Navigate through the file system to the directory where the *app.R* and *helpers.R* files are located. From now on, this will be the working directory and data folders should be copied here for most efficient use of the app.

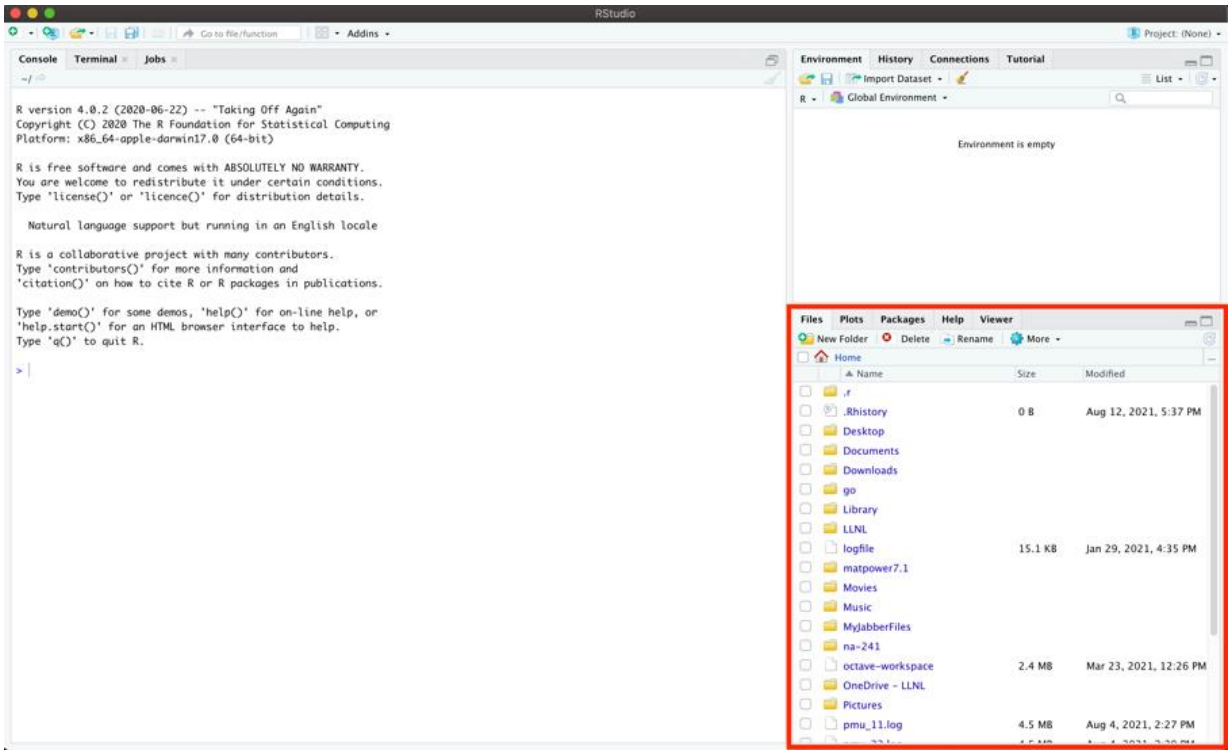

Figure 28 - RStudio initial window.

iii) Click on the *app.R* file and then click the 'run app' button in the top right corner of the source pane, which by default is located in the top left corner of the RStudio window

(Figure 29). If this is the first time running LARA it will initiate the installation of various packages that run within the R-script. This installation process can take several minutes and requires an up-to-date version of the base R-code.

iv) Once loaded, the LARA app will popup. To use the app, navigate to the folder containing the laser ablation data. To do so, click on the "Input directory" button at the top of the window (Figure 30).

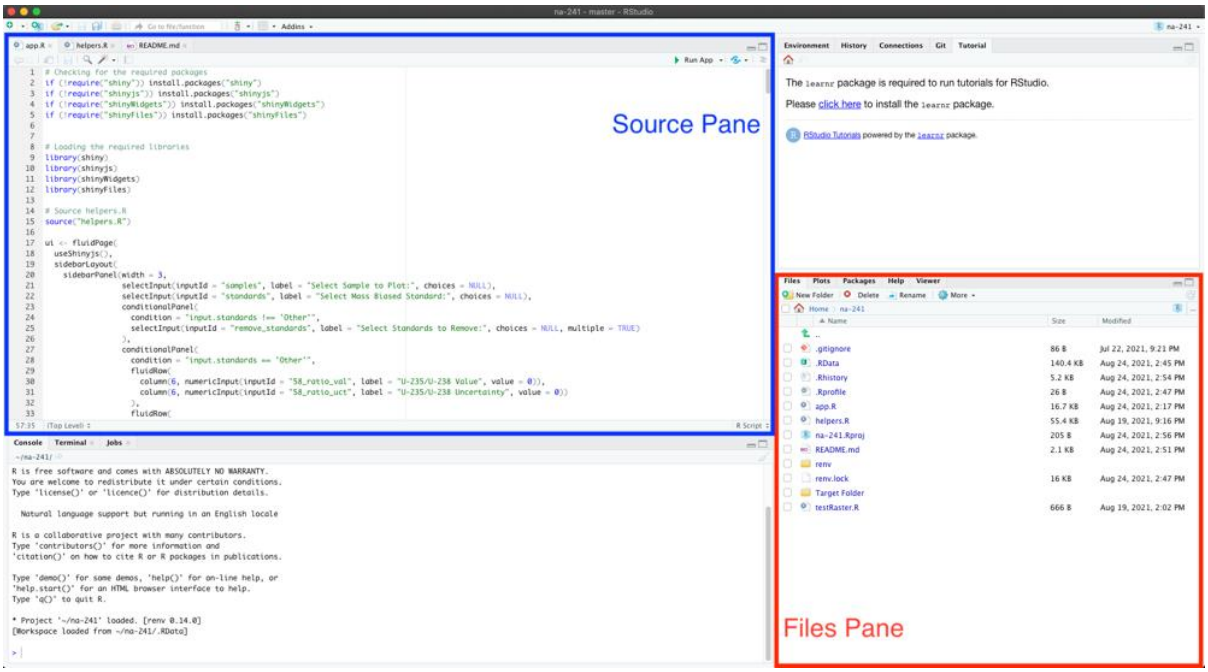

Figure 29 – Source and files panes in R Studio

v) Navigate to the directory where the experiment files are located using the left-hand panel. The right panel simply displays the contents of each folder. Once the folder containing the data is identified click the "Select" button.

vi) LARA will load and plot the raw data for the specified experiment. In the "Select Sample to Plot" dropdown menu, the user can select the specific sample or standard that they want to visualize. This will show the raw data plot for that sample or standard (Figure 31). This plot is interactive, and the user can select or deselect plots of interest. To access the plot functionality simply hover the cursor over the plot and a menu bar will pop-up in the top right.

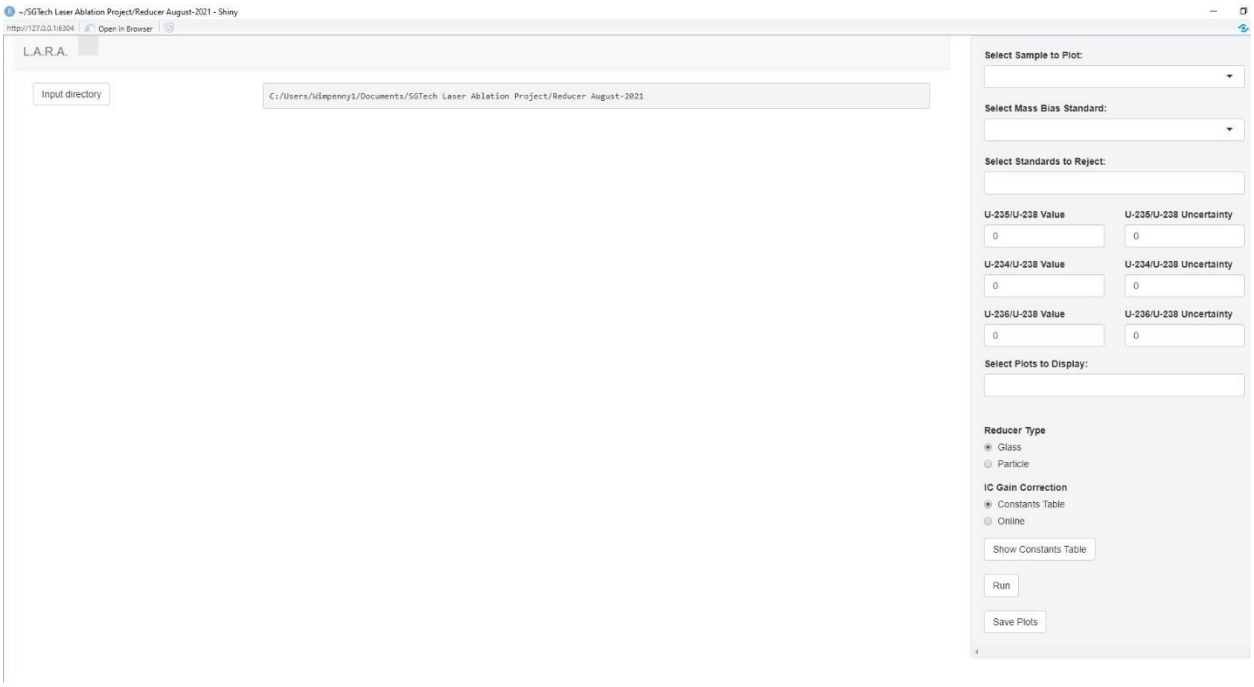

Figure 30 – Initial LARA window.

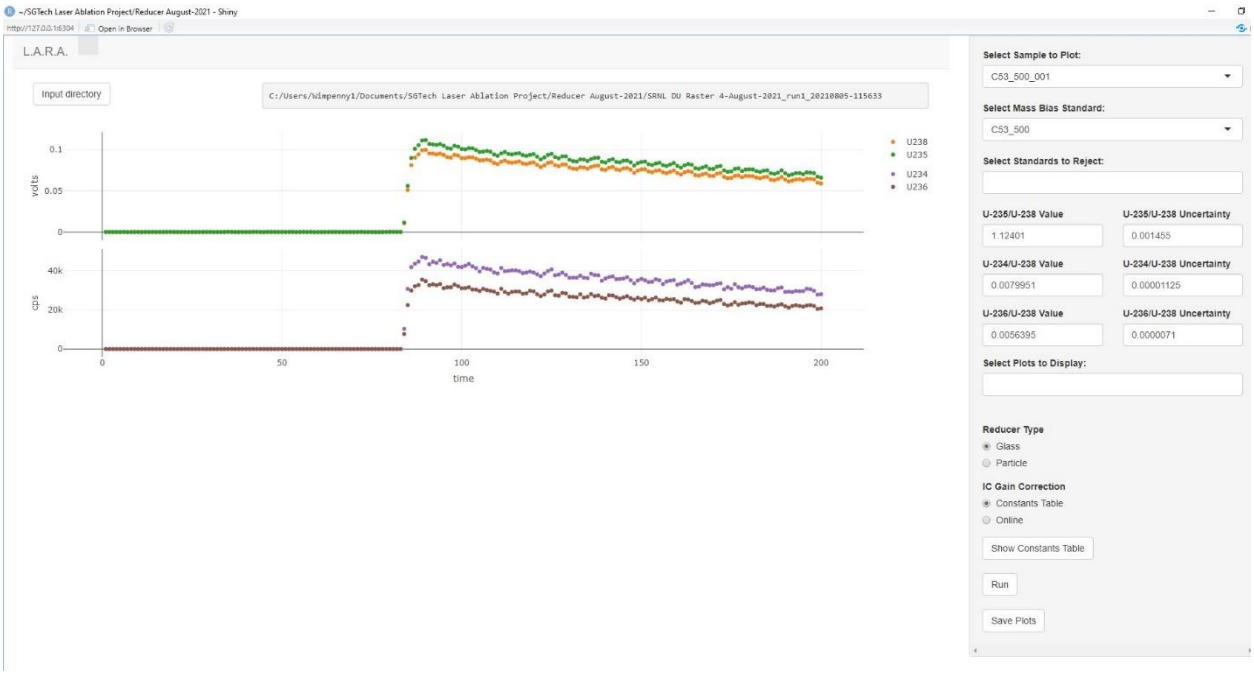

Figure 31 – After loading the raw U isotope data the user can select the plot from individual analysis of standards or samples.

vii) Next, the user identifies which reference standard they want to use for mass bias and ion counter gain corrections using the 'Select Mass Bias Standard' dropdown menu. If one of the default standards was used during the experiment it can be selected and the isotopic composition of that standard (and uncertainties) will populate in the window. The user can change these default values if required (for example, if an updated U isotopic composition has been published). If the experiment used a reference standard that is not included in LARA the user must enter the isotopic compositions in the space provided prior to running the reducer.

viii) The user can remove any individual standard analysis by using the 'Select Standards to Reject' dropdown. This prevents a bad analysis of the reference standard from being propagated into the calculation of the unknowns.

ix) The user can select the reducer type; either 'glass' or 'particle'. In this case, the glass reduction mode is appropriate for reduction of any solid sample with relatively homogenous isotopic composition.

x) The user selects whether the ion counter gains are corrected online or using the gain factors entered in the constants table. These gain factors can be manually updated by the user by simply clicking on the entry to update. To save the change requires clicking ctrl-enter.

xi) Once all of the options have been selected the user clicks on 'run' at the bottom right-hand side of the reducer pane.

xii) The application will notify the user while the code is running and when it is finished with messages that popup in the right-hand corner. The reduced U-isotope data will be automatically exported in .csv format into the specified directory.

xiii) The application will produce $^{234}U/^{238}U$, $^{235}U/^{238}U$ and $^{236}U/^{238}U$ plots for the selected sample, as illustrated in Figure 32.

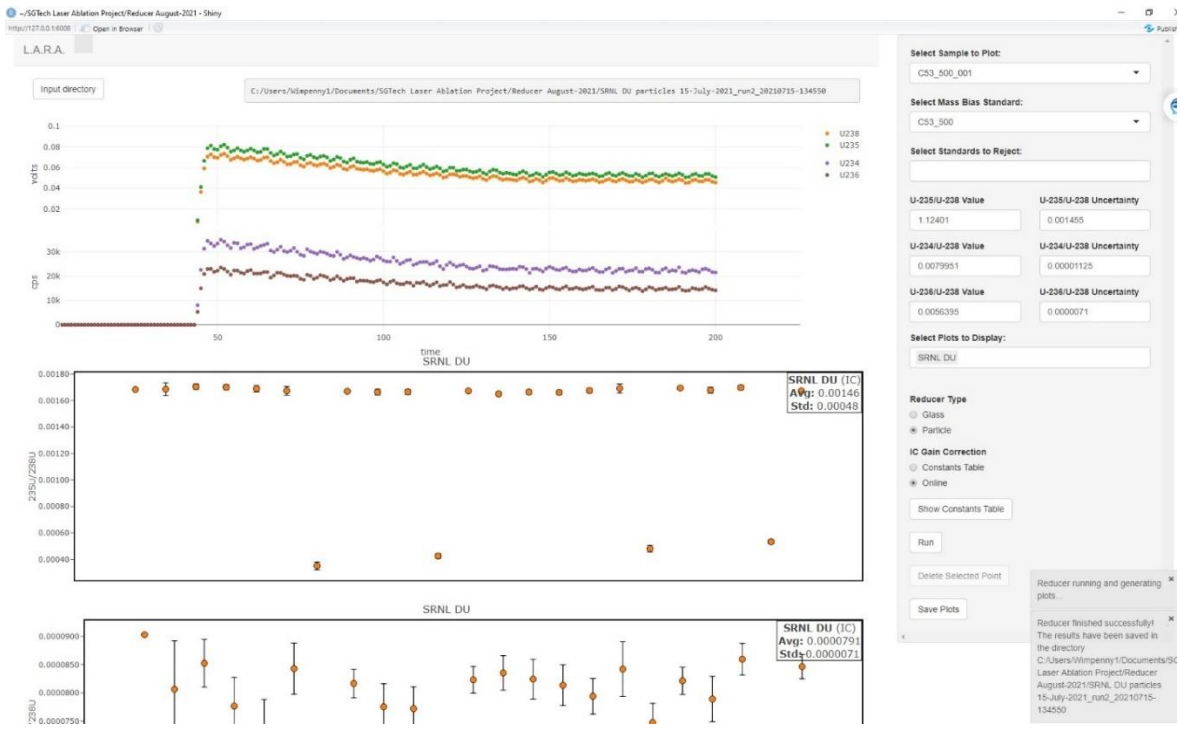

Figure 32 – After the reducer has run, LARA will generate U isotope plots for the selected sample.

xiv) Each of the plots will show the average and standard deviation of the isotope ratio from a specific sample. Any samples that need to be rejected can be identified and excluded here. To do this, the user hovers over the plot with the outlying data point. Select 'box select' under the popup menu in the top right of the plot and draw a box around the outlying sample point. The button 'delete selected point' becomes active and can be used to delete this point. All three U isotope plots ($^{235}U/^{238}U$, $^{234}U/^{238}U$ and $^{236}U/^{238}U$) are updated with removal of the selected data point. Final plots can be saved individually using the built-in save plot option in the popup menu. For a more user-friendly experience, a 'Save Plots' button is available to save all plots at once with just one click. The save plots option requires installation of the Orca command line utility (https://github.com/plotly/orca#installation).

xv) LARA will show notification banners on the bottom right corner when all of the plots are saved (specifying the destination directory).

xvi) To reduce another data set the user can simply repeat these steps after selecting the new data folder.

7.7. Current limitations to the LARA interface

LARA is a highly capable platform from which uranium isotopic data obtained by laser ablation can be reduced and uncertainties propagated. However, there are limitations to the current program that any external user should be aware of. The most important of which is that the program is limited to handling data with a set structure. This means that LARA cannot be used to reduce isotopic data from different elements such as plutonium; it is currently only compatible with uranium. Perhaps more importantly, the current data structure is different to that generated by single collector ICP-MS instruments (e.g. Thermo Element XR HR-ICP-MS, Thermo iCAP q-ICP-MS) and MC-ICP-MS instruments manufactured by Nu Instruments. This means that, without further development, LARA is currently only compatible with laser ablation analysis performed using the Thermo Neptune MC-ICP-MS.

We have also identified several minor modifications that could be made to improve the program. These include providing an option to save any modifications to the constants table (currently this resets to the hard coded values every time the program starts), addition of standard information for a wider range of U reference materials, providing a hyperlink to the data folder where the exported .csv file is saved and other cosmetic tweaks to the plotting.

Although these are limitations to the code, the basic architecture is in place that controls how data is handled, reduced and uncertainties propagated. In other words, much of the hard work in development has already been completed. Should the IAEA, or any other end user, require data to be processed with a different structure would require relatively straightforward modifications to the code. We envisage that several user-selected options regarding the element analyzed (e.g. uranium or plutonium) and the instrument selection (e.g. Neptune or Element XR) would be provided prior to the selection of the data folder. These would simply control how the data is identified and how the raw data plots are presented. The reduction of the isotopic data following this would then proceed similarly to the way data is handled by the current code.

8. Summary

The goal of this project was to stand up the laser ablation MC-ICP-MS technique for direct measurement of U isotope ratios in micron-scale particles. In this report, we detailed our method development, beginning with setup of the hardware, then testing the accuracy of U isotope ratio measurements in reference glasses, before moving onto characterizing U-particle samples. In addition, we also detailed a robust isotopic data reduction package using an application designed in R.

Results of testing show that we can achieve accurate U isotope ratio data for both glass and particle samples. Glasses have relatively homogenous U concentrations and isotopic compositions, leading to relatively high precision data. Typical precision of the $^{235}U/^{238}U$ ratio is better than 0.5%, irrespective of glass composition, with ratios accurate to within 1.7%. Minor isotope data is of mixed quality in glasses with natural or depleted $^{235}U/^{238}U$ ratios (due to correspondingly low ^{234}U and ^{236}U contents). However, in glasses with 50-90% ^{235}U we were able to obtain accurate and precise $^{234}U/^{238}U$ and $^{236}U/^{238}U$ ratios to within ~1% of reference values.

The ablation of micron scale U-particles is more challenging due to the limited and short-lived U signal generated by each particle. Despite this, our results show that laser ablation MC-ICP-MS is a rapid and accurate method to characterize their isotopic compositions. Replicate analyses of 49 particles of the reference standard U200 produced $^{235}U/^{238}U$ ratios that were within uncertainty of reference values, with a precision of ~2.5%. We were also able to obtain accurate minor isotope ratios from particles of U200, with precision within ~6%. The data quality achieved from particles of depleted uranium (SRNL-DU) depended on the detector used to collect ^{235}U data (Faraday or Ion Counter). Final $^{235}U/^{238}U$ ratios from both detectors were similar ($^{235}U/^{238}U$ ~0.0016) and within uncertainty of the reference composition obtained by LG-SIMS (Table 11). However, with ^{235}U on IC the precision is ~1.8%, whereas this drops to ~80% using a Faraday detector. This large uncertainty is simply a function of operating near the detection limit of the Faraday cup in samples that have highly depleted ^{235}U contents. Ultimately, the testing completed here shows that we can achieve %-level precision on the $^{235}U/^{238}U$ ratio from micron sized U-particles using laser ablation MC-ICP-MS. Unexpectedly, the technique is sensitive enough to also produce $^{234}U/^{238}U$ and $^{236}U/^{238}U$ ratios that closely match ratios and uncertainties produced by LG-SIMS (Table 11). Testing on SRNL-DU demonstrates that we can resolve ^{234}U contents <10ppm and ^{236}U contents <80ppm in micron-scale particles of uranium. This indicates that laser ablation MC-ICP-MS could be a viable alternative to LG-SIMS for future Safeguards purposes.

Finally, the design of a robust data reduction package in R allows the fast and reliable reduction of U isotope data produced by laser ablation. This is a vital aspect of developing the technique for future use by the IAEA. By rastering the laser over the silicon planchet we are able to obtain data from tens to hundreds of particles in a timeframe of minutes to hours. The advantages of such rapid data collection are that high priority samples can be analyzed quickly and that it will increase total sample throughput. These gains become irrelevant if the data cannot be processed equally quickly. We have laid out the architecture required to handle time resolved data and propagate uncertainties in a user-friendly interface. Further development of the app to enhance functionality and flexibility may be required in the future.

Ultimately, this project has highlighted that laser ablation MC-ICP-MS can be a fast and reliable technique to characterize the isotopic composition of samples relevant to IAEA safeguards. The data quality obtained from analyses of depleted uranium particles is comparable

to that obtained from LG-SIMS. The work documented here supports the continued development of particle analysis by laser ablation for the IAEA-NWAL and the potential integration of this technology into mission operations.

Table 11 – Comparison between U isotope data for the SRNL-DU particle sample obtained by laser ablation MC-ICP-MS and LG-SIMS (see caption to Table 10 for more details). Uncertainties are 2σ. *Reference values from LG-SIMS analysis are provided from Scott et al., (2021).

Isotopic composition	**$^{234}U/^{238}U$**	**2σ**	**$^{235}U/^{238}U$**	**2σ**	**$^{236}U/^{238}U$**	**2σ**
Laser Ablation (^{235}U IC2)	0.0000071	0.0000025	0.001677	0.000030	0.000078	0.000014
Laser Ablation (^{235}U L5)			0.0016	0.0013		
LG-SIMS (single particle)*	0.0000068	0.0000035	0.00173	0.00010	0.0000807	0.0000086
LG-SIMS (particle mapping)*	0.0000088		0.00174		0.000079	

9. References

Craig, G., Horstwood, M. S., Reid, H. J., & Sharp, B. L. (2020). 'Blind time'–current limitations on laser ablation multi-collector inductively coupled plasma mass spectrometry (LA-MC-ICP-MS) for ultra-transient signal isotope ratio analysis and application to individual sub-micron sized uranium particles. Journal of Analytical Atomic Spectrometry, 35(5), 1011-1021.

Donard, A., Pointurier, F., Pottin, A. C., Hubert, A., & Pécheyran, C. (2017). Determination of the isotopic composition of micrometric uranium particles by UV femtosecond laser ablation coupled with sector-field single-collector ICP-MS. Journal of Analytical Atomic Spectrometry, 32(1), 96-106.

Duffin, A. M., Hart, G. L., Hanlen, R. C., & Eiden, G. C. (2013). Isotopic analysis of uranium in NIST SRM glass by femtosecond laser ablation MC-ICPMS. Journal of Radioanalytical and Nuclear Chemistry, 296(2), 1031-1036.

Duffin, A. M., Springer, K. W., Ward, J. D., Jarman, K. D., Robinson, J. W., Endres, M. C., ... & Willingham, D. G. (2015). Femtosecond laser ablation multicollector ICPMS analysis of uranium isotopes in NIST glass. Journal of Analytical Atomic Spectrometry, 30(5), 1100-1107.

Eppich, G. R., Wimpenny, J. B., Leever, M. E., Knight, K. B., Hutcheon, I. D., and Ryerson, F. J. Characterization of low concentration uranium glass working materials. United States: N. p., 2016. Web. doi:10.2172/1254390.

Jochum, K. P., Wilson, S. A., Abouchami, W., Amini, M., Chmeleff, J., Eisenhauer, A., ... & McDonough, W. F. (2011). GSD-1G and MPI-DING reference glasses for in situ and bulk isotopic determination. Geostandards and Geoanalytical Research, 35(2), 193-226.

Knight K, Wimpenny J, Weber P, Willingham D & Groopman E (2018) Goldschmidt Abstracts, 2018 1315.

Müller, W., Shelley, M., Miller, P., & Broude, S. (2009). Initial performance metrics of a new custom-designed ArF excimer LA-ICPMS system coupled to a two-volume laser-ablation cell. Journal of Analytical Atomic Spectrometry, 24(2), 209-214.

Pointurier, F., Pottin, A. C., & Hubert, A. (2011). Application of nanosecond-UV laser ablation–inductively coupled plasma mass spectrometry for the isotopic analysis of single submicrometer-size uranium particles. Analytical chemistry, 83(20), 7841-7848.

R Core Team, 2017. R: A Language and Environment for Statistical Computing. R Foundation for Statistical Computing, Vienna, Austria. URL https://www.R-project.org/

Richter, S., & Goldberg, S. A. (2003). Improved techniques for high accuracy isotope ratio measurements of nuclear materials using thermal ionization mass spectrometry. International Journal of Mass Spectrometry, 229(3), 181-197.

Ronzani, A. L., Hubert, A., Pointurier, F., Marie, O., Clavier, N., Humbert, A. C., ... & Dacheux, N. (2019). Determination of the isotopic composition of single sub-micrometer-sized uranium particles by laser ablation coupled with multi-collector inductively coupled plasma mass spectrometry. Rapid Communications in Mass Spectrometry, 33(5), 419-428.

Scott, S. M., Baldwin, A. T., Bronikowski, M. G., DeVore II, M. A., Inabinet, L. A., Kuhne, W. W., Naes, B. E., Smith, R. J., Villa-Aleman, E., Tenner, T. J., Wurth, K. N., & Wellons, M. S., (2021) Scale-up And Production Of Uranium-bearing QC Reference Particulates By An Aerosol Synthesis Method. *INMM Annual Meeting Proceedings*, 2021.

Xu, L., Hu, Z., Zhang, W., Yang, L., Liu, Y., Gao, S., ... & Hu, S. (2015). In situ Nd isotope analyses in geological materials with signal enhancement and non-linear mass dependent fractionation reduction using laser ablation MC-ICP-MS. *Journal of Analytical Atomic Spectrometry*, *30*(1), 232-244.

Zimmer, M. M., Kinman, W. S., Kara, A. H., & Steiner, R. E. (2014). Evaluation of the homogeneity of the uranium isotope composition of NIST SRM 610/611 by MC-ICP-MS, MC-TIMS, and SIMS. *Minerals*, *4*(2), 541-552.

10. Appendix

Appendix A – $^{238}U/^{235}U$ data produced for the reference standards GSD-1G, NIST 610 and NIST 612 in a single analytical sequence. Uncertainties are 2σ (standard error). No correction for IC2-Faraday gain is applied to these data.

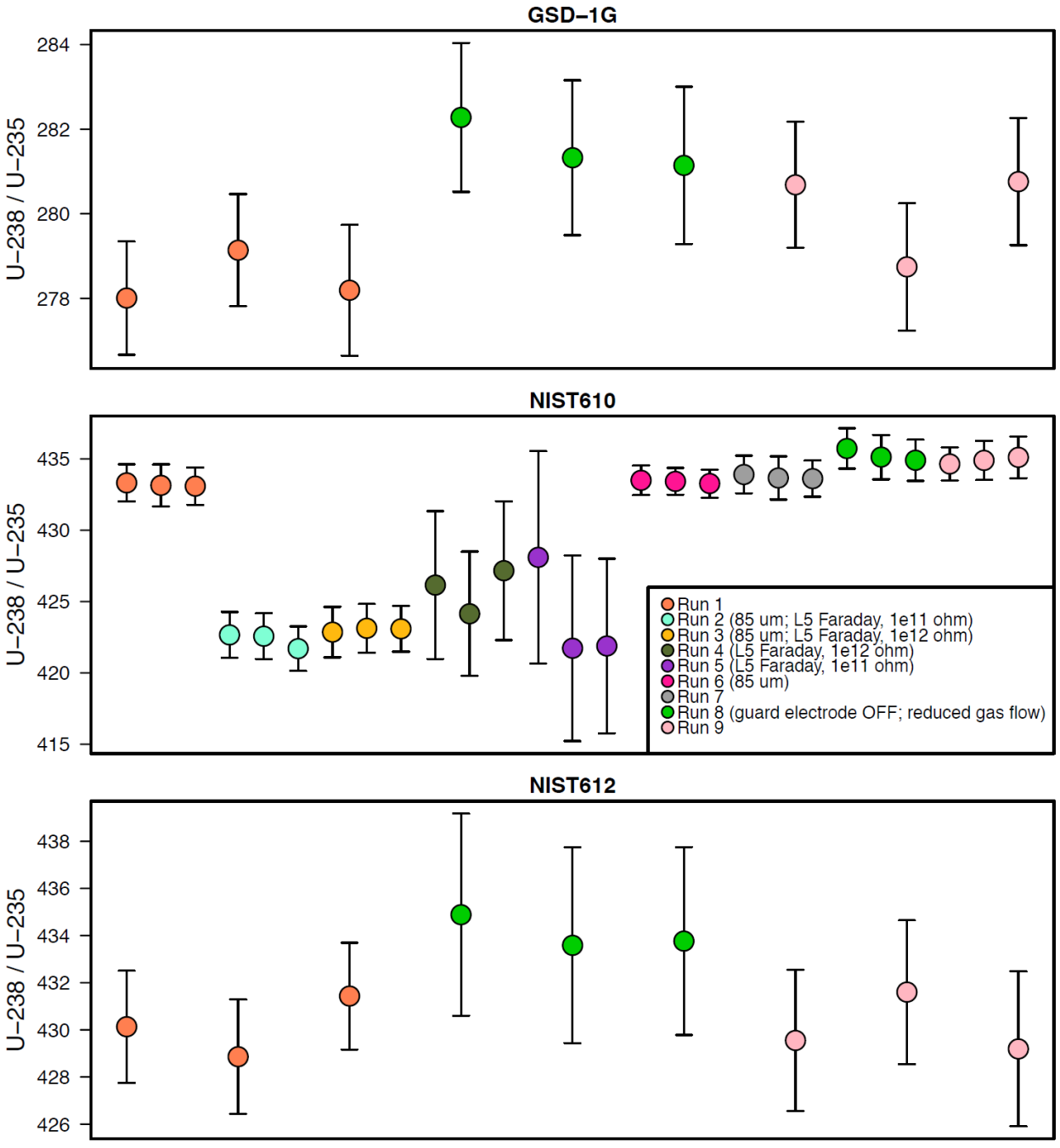

Appendix B - $^{234}U/^{235}U$ data produced for the reference standards GSD-1G, NIST 610 and NIST 612 in a single analytical sequence. Uncertainties are 2σ (standard error).

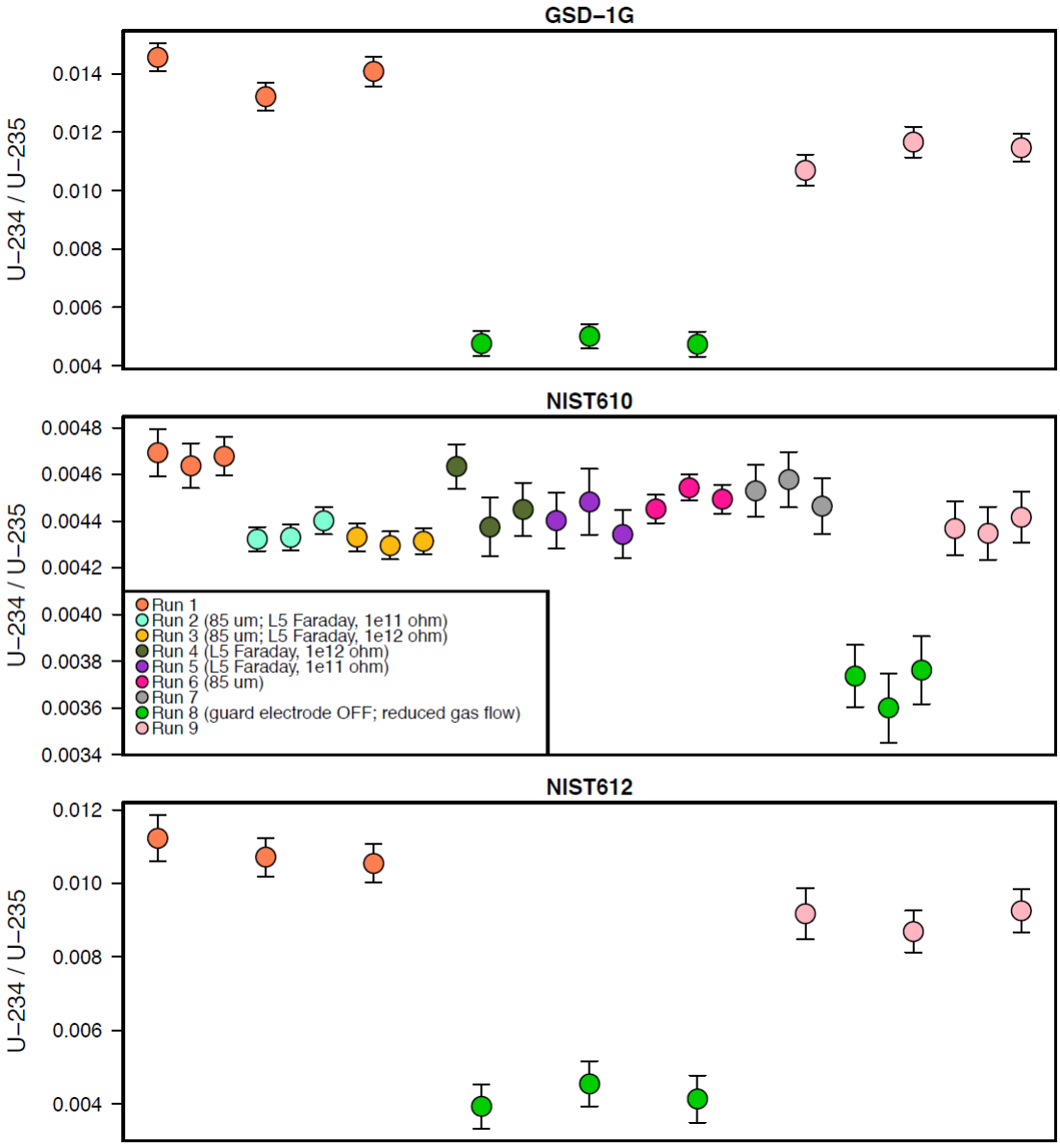

Disclaimer

Lawrence Livermore National Laboratory is operated by Lawrence Livermore National Security, LLC, for the U.S. Department of Energy, National Nuclear Security Administration under Contract DE-AC52-07NA27344.